Robust Longitudinal Control of a Platoon of Vehicles Based on Adaptive Fuzzy Neural Approach

:

:

Robust Longitudinal Control of a Platoon of Vehicles Based on Adaptive Fuzzy Neural Approach

Student　Yung-Chien Fan

Advisors　Lon-Kou Chang

Tsu-Tian Lee

H_∞

H_∞

Robust Longitudinal Control of a Platoon of Vehicles Based on Adaptive Fuzzy Neural Approach

Student　Yung-Chien Fan　　　　Advisors　Lon-Kou Chang

Tsu-Tian Lee

Department of Electrical and Control Engineering
National Chiao Tung University

Abstract

In this Thesis, three different controllers for the longitudinal car following system, including a fuzzy logic controller, a sliding mode controller , and a sliding-observer-based sliding mode controller with indirect adaptive fuzzy neural network approximator and H_∞ performance, are proposed. For a longitudinal control of a platoon of a vehicles in a straight line, as the speed of the preceding vehicle increases or decreases, the relative distance of vehicles changes. This will be used to act the throttle (or brake) of the follow vehicle. The main control strategy is to force the follow vehicle tracking the lead one with a safety distance. We assume that the relative distance is measurable and measured by the follow vehicle.

The fuzzy logic controller for a longitudinal car-following system provides a good performance for the follow vehicle to track the lead one. The sliding mode controller provides more stable and reliable performance. After associating with the fuzzy neural network approximator and H_∞ performance, the controller performs as well as the sliding mode controller and meanwhile smooth the control actions. Under the assumption that only the relative distance is measurable, the sliding observer is combined with the former controller. It also guarantees the overall system is globally stable. Simulation results will show the validity and effectiveness of the proposed controllers.

Keywords　car-following, adaptive control, sliding mode control, sliding observer, fuzzy logic control, fuzzy-neural network

Contents

List of Tables

List of Figures

Chapter 1 Introduction

1.1 Motivations

Recently, collision prevention and high traffic flow are the key technologies for the intelligent vehicle highway system (IVHS) to control traffic congestion. In order to achieve these goals, much effort has been spent on various control laws for automated highway system (AHS) in which high traffic flow rates may be safely achieved. One way to carry out these objectives in the car-following system of the AHS is to decrease the inter-vehicular spacing and keep it in a safety distance, that is, we are concerned about the safe separation of automatic vehicles in a platoon of vehicles when the preceding vehicle is accelerating or decelerating. Moreover, because of the variation of vehicle mass – the sum of curb mass and passengers' mass, and of the variant properties of different types of vehicles, passengers may take a lot of risks in the car-following period. Thus, a stable and reliable controller is needed.

1.2 Literatures Survey

Up to now, many researches are studied for longitudinal control of vehicle systems [1, 7-8, 12, 14-15, 18]. Among these researches, a more detailed discussion of the vehicle model is to be found in section 2.1 and 2.2 adopted from [1].

Over the past decade, fuzzy logic controller (FLC) has been successfully applied to many control problems [20-21, 28]. Because FLC contains linguistic information to model the qualitative aspects of human knowledge, it can be designed based on deficient knowledge about the complex controlled system. Since FLC can overcome the environmental variation during the movements of vehicles, many FLC are developed and implemented in many autonomous vehicle control systems [22-23, 34-36]. Besides, the control actions are smoothed through the well-built control rules. However, the global stability of FLC has also been questioned.

Sliding mode control method is frequently used in many control systems because of its capability of dealing with uncertain systems, robustness under parameter variations, fast convergence speed, etc. In order to ensure global stability of the vehicle systems, we propose the controlled plant using a sliding mode controller in the thesis. However, there are two disadvantages – system dynamics must be exactly known and the control chattering occurs.

To solve the disadvantage of the former, we adopt a fuzzy neural network approximator to approach the nonlinear unknown part of dynamics. Parallel to the development of FLC, neural networks are also applied to several control problems. Because both the neural network and fuzzy logic system are universal approximators, researches have been conducted to derive various fuzzy neural network controllers. A

direct and indirect adaptive control schemes using fuzzy systems and neural networks

for nonlinear systems is proposed [19]. Moreover, researches augmented the sliding

mode method with fuzzy logic systems or neural network or both are proposed

[29-31].

To solve the disadvantage of the latter in this thesis, one way is to use the

boundary layer [11], and the other way is to adopt H_∞ tracking design technique

[9-10].

In reality, however, utilizing some detecting sensors may be difficult or

expensive to obtain accurate information of system states. Thus, the estimations of

states from system output are required. Some kinds of observers are proposed [24,

32-33].

1.3 Thesis Organizations

The remainder of the thesis is organized as follows. In Chapter 2, the vehicle

model and the configuration of a platoon of vehicles are described. Chapter 3

introduces the fuzzy logic controller followed by the simulation results. In Chapter 4,

four classes of controllers – a sliding mode controller, a sliding mode controller based

on fuzzy neural approach, a sliding mode controller with the fuzzy neural approach

and H_∞ performance, and H_∞-observer-based sliding mode controller with the

fuzzy neural approximator are introduced respectively and the simulation results are

shown in the section 4.6. Lastly, conclusions are included in Chapter 5.

Chapter 2   Descriptions of Vehicle Model and a Platoon

of Vehicles

In this chapter, the platoon model and the longitudinal vehicle model will be introduced. Incorporated with different controllers proposed in the following chapters, the model is conducive to evaluate the performance of the designed longitudinal car following collision prevention system.

Thereinafter, we will illustrate a platoon of vehicles with no communication of lead vehicle, and then make a description about the transformation from a tracking problem to a regulator problem. Considering the vehicle engine power is limited in reality, we mention the reasonable range of the throttle of the vehicle finally.
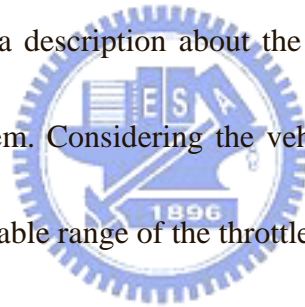
2.1 A Platoon of *N* Vehicles

Consider a platoon of *N* automotive vehicles on a straight lane of a highway, described in Fig. 2-1 [1]. The platoon is assumed to move from left to right. The abscissa of the rear bumper of the *i*th vehicle with respect to a fixed reference point *O* on the road is denoted by x_i. The position of the lead vehicle's rear bumper with respect to the same fixed reference point is denoted by x_l. Safety distance between every two vehicles is assigned a slot of length *L* along the road. As Shown, for *i=1,2,...,N*, Δ_i denotes the deviation of *i*th vehicle position from its assigned

position. The subscript i is used because Δ_i is measured by the sensors located in the ith vehicle. Given the platoon configuration in Fig. 2-1, elementary geometry shows that :

$$\Delta_1 = x_l - x_1 - L$$

$$\Delta_i = x_{i-1} - x_i - L \qquad , i=2,3,...,N \qquad (2.1)$$

We assume that Δ_i is measured in the vehicle i and , together with its first and second derivatives, is used in the ith vehicle's control law. The behavior of ith vehicle is related to the preceding vehicle's information via sensors but not with communication. It is safer in the longitudinal control for collision prevention because it is unconcerned about loss of communication between the lead vehicle and the other vehicles in the platoon.
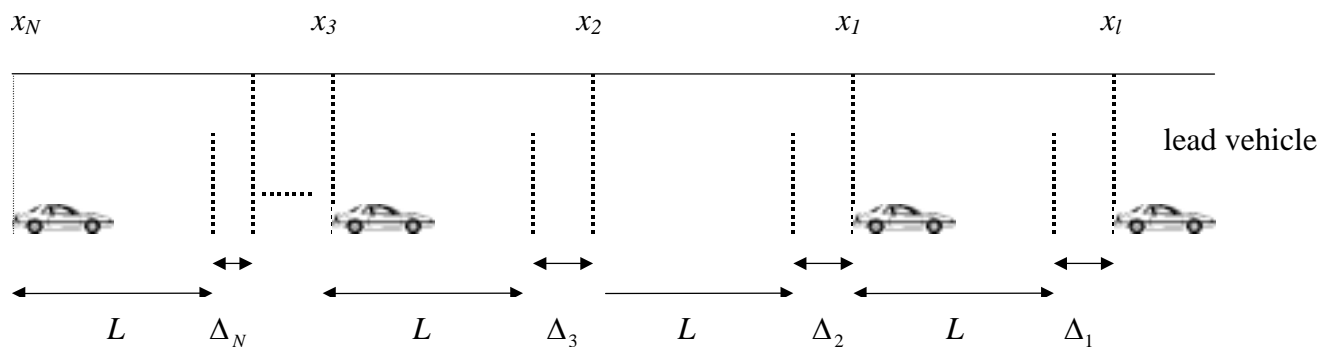
Fig. 2-1 Configuration of A Platoon of N Vehicles

2.2 Vehicle Model

We assume that the road is horizontal, there is no wind gust, and all the vehicles travel in the same direction at all times. Fig. 2-2 shows the simplified vehicle model of the ith vehicle in the platoon. The block ($K_{di}\dot{x}_i^2$) specifies the force due to the air resistance, where K_{di} denotes the aerodynamic drag coefficient for the ith vehicle $\rho A_i C_{di}/2$, ρ denotes the specific mass of air, A_i denotes the cross-sectional area of the ith vehicle, and C_{di} denotes the ith vehicle's drag coefficient; F_i denotes the driving force produced by the ith vehicle's engine; m_i denotes the mass of the ith vehicle; u_i denotes the throttle command input to the ith vehicle's engine; and k_{mi} denotes the ith vehicle's mechanical drag. The longitudinal dynamics of the ith vehicle in the platoon are modeled as follows (for $i=1,2,...,N$) [1]:

$$\dot{F}_i = -\frac{F_i}{\tau_i(\dot{x}_i)} + \frac{u_i}{\tau_i(\dot{x}_i)} \tag{2.2}$$

$$m_i\ddot{x}_i = F_i - K_{di}\dot{x}_i^2 - k_{mi} \tag{2.3}$$

where $\tau_i(.)$ denotes the engine time lag for the ith vehicle. Equation (2.2) described by a nonlinear differential equation represents the ith vehicle's engine dynamics, and (2.3) represents Newtons's second law applied to the ith vehicle modeled as a particle of mass m_i.

Differentiating both sides of (2.3) with respect to time, we have

$$m_i\dddot{x}_i = \dot{F}_i - 2K_{di}\dot{x}_i\ddot{x}_i \tag{2.4}$$

Substituting the expression for $\dot{F}_i$ by (2.2), (2.4) becomes

$$m_i \dddot{x}_i = -\frac{F_i}{\tau_i(\dot{x}_i)} + \frac{u_i}{\tau_i(\dot{x}_i)} - 2K_{di}\dot{x}_i\ddot{x}_i \tag{2.5}$$

from (2.3) and (2.5) we obtain

$$\dddot{x}_i = -\frac{1}{\tau_i(\dot{x}_i)}\left[\ddot{x}_i + \frac{K_{di}}{m_i}\dot{x}_i^2 + \frac{k_{mi}}{m_i}\right] - \frac{2K_{di}}{m_i}\dot{x}_i\ddot{x}_i + \frac{1}{m_i\tau_i(\dot{x}_i)}u_i \tag{2.6}$$

where $\dddot{x}_i$ denotes the variation of the ith vehicle's acceleration.

Let $x_i = p_i$, $\dot{x}_i = v_i$, and $\ddot{x}_i = a_i$. The longitudinal ith vehicle dynamics can be written as

$$\begin{cases} \dot{p}_i = v_i \\ \dot{v}_i = a_i \\ \dot{a}_i = f_i(v_i, a_i) + g_i(v_i)u_i \end{cases} \tag{2.7}$$

where

$$f_i(v_i, a_i) = -\frac{1}{\tau_i(v_i)}\left[a_i + \frac{K_{di}}{m_i}v_i^2 + \frac{k_{mi}}{m_i}\right] - \frac{2K_{di}}{m_i}v_i a_i \quad \text{and}$$

$$g_i(v_i) = \frac{1}{m_i\tau_i(v_i)}$$

The control objective is to keep ith vehicle follow it's preceding vehicle and hold on a secure distance L, that is, $x_l - x_1 = L$, $x_1 - x_2 = L, \ldots$, and $x_{N-1} - x_N = L$. Namely, to input throttle command u_i such that Δ_i can be driven to zero. At the same time, $\dot{\Delta}_i$ and $\ddot{\Delta}_i$ are driven to zero, too. Meanwhile, we have changed a tracking problem to a regulator problem.
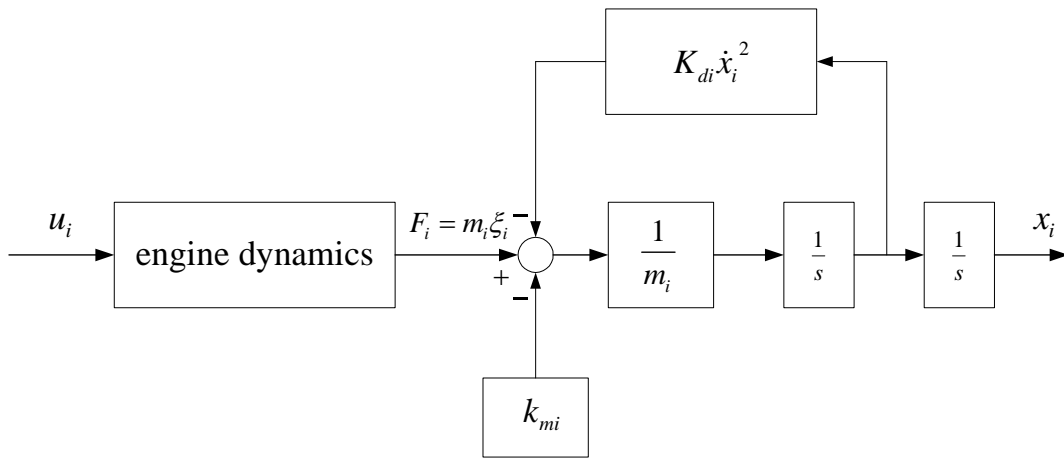
Fig. 2-2 Simplified model of the *i*th vehicle in the platoon

2.3 Power-Limited Acceleration

Maximum performance in longitudinal acceleration of a motor vehicle is determined by lots of limits; engine power is one of the most important factors of these limits. Fig. 2-3 [4] shows the performance characteristics of gasoline engine. Power and torque are related by the speed. Specifically,

$$\text{HorsePower(hp)} = \text{Torque(ft-lb)} \times \text{Speed(rpm)} \div 5252 \qquad (2.8)$$

Also,

$$\text{Power(kw)} = 0.746 \times \text{HorsePower(hp)} \qquad (2.9)$$

Thus, we obtain the reasonable range of u_i is within 4000 N. Practically, with the advance of science and technology, maximum engine power limit is higher today.

9
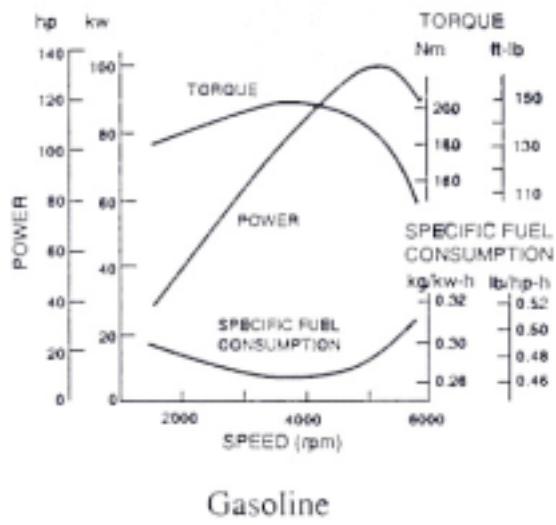
Fig. 2-3 Performance characteristics of gasoline engine [4]

Chapter 3   Fuzzy Logic Control

Fuzzy logic control is a useful methodology for system control in the presence of uncertainties and disturbances. The independence of expert knowledge of the controlled plants is a remarkable advantage in fuzzy logic controller (FLC) design. Besides, the control actions are usually smoothed through the well-built control rules. The basic principles of fuzzy logic were introduced by Zadeh in 1965, and the first application to the control of a dynamical process was reported by Mamdani in 1975. Because of the advantages such as easy implementation, suitability for complex dynamic systems, and high flexibility and robust nature, fuzzy controllers have been implemented in many fields [24-26].

The characteristic of FLC is that it adopts the linguistic control strategy to control plants without realizing their mathematical models. The linguistic control strategy of FLC is constructed according to the operator experience and/or expert knowledge. Experiences show that the FLC yields results superior to those obtained by traditional control algorithm in the complex situation where the system model or parameters are difficult to obtain.

Typically, fuzzy controllers are based on four well-known stages: a fuzzification interface, a rule base, an inference engine, and a defuzzification interface as shown in Fig. 3-1. More detail descriptions for each stages are stated below.
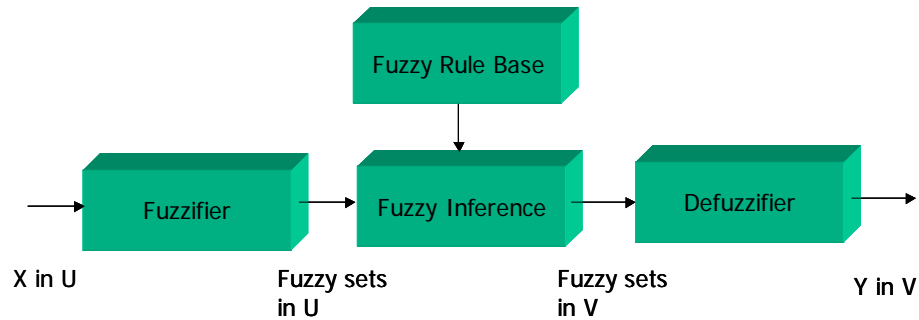
Fig. 3-1 Fuzzy System Architecture

3.1 Fuzzy Set and Set-Theoretical Operators

Definition 3.1 *Fuzzy Set*: Let *U* be a collection of objects, for example, $U = R^n$, and be called the universe of discourse. A fuzzy set *F* in *U* is characterized by a membership function $\mu_F : U \to [0,1]$, with $\mu_F(u)$ representing the grade of membership of $\mu \in U$ in the fuzzy set *F*.

Definition 3.2 *Support, Fuzzy Singleton*: The support of a fuzzy set *F* is the point(s) $u \in U$ at which $\mu_F(u)$ achieves its maximum value. If the support of a fuzzy set *F* is a single point in *U* at which $\mu_F = 1$, the *F* is called a fuzzy singleton.

Definition 3.3 *Intersection, Union, and complement*: Let A and B be two fuzzy sets in *U*. The intersection $A \cap B$ of A and B is a fuzzy set in *U* with a membership function defined for all $u \in U$ by

$$\mu_{A \cap B}(u) = \min\{\mu_A(u), \mu_B(u)\} \tag{3.1}$$

The union of $A \cup B$ of A and B is a fuzzy set in *U* with the membership defined for all $u \in U$ by

12

$$\mu_{A \cup B}(u) = \max\{\mu_A(u), \mu_B(u)\} \tag{3.2}$$

Usually, the intersection and union operators are denoted by $\wedge$ and $\vee$, respectively. The complement $\overline{A}$ of A is a fuzzy set in U with the membership function defined for all $u \in U$ by

$$\mu_{\overline{A}}(u) = 1 - \mu_A(u) \tag{3.3}$$

3.2 Fuzzifiers

The fuzzifier stage transforms crisp input from real values into fuzzy sets. Here we introduce three fuzzifiers as following:

1. Singleton fuzzifier: the singleton fuzzifier maps a real valued point $x^* \in U$ into the fuzzy singleton A in U, in which the membership value is 1 at x^* and 0 at other points in U, i.e.,

$$\mu_A(x) = \begin{cases} 1 & x = x^* \\ 0 & \text{otherwise} \end{cases} \tag{3.4}$$

2. Triangular fuzzifier: the triangular fuzzifier maps $x^* \in U$ into the fuzzy set A in U, in which the membership function is written as:

$$\mu_A(x) = \begin{cases} (1 - \dfrac{|x_1 - x_1^*|}{b_1}) \otimes \cdots \otimes (1 - \dfrac{|x_n - x_n^*|}{b_n}) & \text{if } |x - x^*| < b_i, i = 1,2,\ldots n \\ 0 & \text{otherwise} \end{cases} \tag{3.5}$$

where b_i are positive parameters and symbol $\otimes$ is often chosen as algebraic product or minimum.

3. Gaussian fuzzifier: the Gaussian fuzifier maps $x^* \in U$ into the fuzzy set A in U, in

13

which the membership function is written as:

$$\mu_A(x) = e^{-(\frac{x_1 - x_1^*}{\delta_1})^2} \otimes \cdots \otimes e^{-(\frac{x_n - x_n^*}{\delta_n})^2} \tag{3.6}$$

where δ_i are positive parameters and symbol $\otimes$ is often chosen as algebraic product

or minimum.

Finally, we summarize the above fuzzifiers. The singleton fuzzifier greatly

simplifies the computation involved in the fuzzy inference engine for all membership

functions. And the Gaussian and triangular fuzzifiers do, too. The Gaussian and

triangular fuzzifiers can restrain noise in the input, but the singleton fuzzifier cannot.

3.3 Deffuzzifiers

The defuzzifier is defined as a mapping from a fuzzy set D in $V \subset R$ to a

crisp point $y^* \in V$. Hence, the task of the defuzzifier is to specify a point in V that

represents the fuzzy set D. There are three types of defuzifiers introduced below.
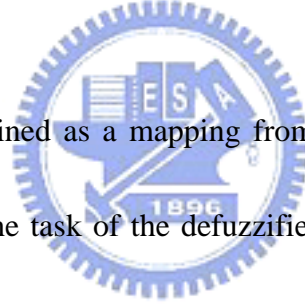
1. Center of gravity Defuzzifier

The center of gravity defuzzifier specifies y^* as the center of the area covered

by the membership function of D.

$$y^* = \frac{\int_V y\mu_D(y)dy}{\int_V \mu_D(y)dy}, \tag{3.7}$$

where $\int_V$ is the conventional integral.

2. Center Average Defuzzifier

Let $\bar{y}^l$ be the center of the lth fuzzy set and w_l be its height. The center

average defuzzifier presents y^* as

$$y^* = \frac{\sum_{l=1}^{M} \bar{y}^l w_l}{\sum_{l=1}^{M} w_l}$$ (3.8)

3. Maximum Defuzzifier

The maximum defuzzifier chooses y^* as the point in V, at which $\mu_D(y)$ achieves its maximum value. Define

$$hgt(D) = \{y \in V \mid \mu_D(y) = \sup_{y \in V} \mu_D(y)\}.$$ (3.9)

$hgt(D)$ is a set of all point in V, at which $\mu_D(y)$ achieves its maximum value. The maximum defuzzifier y^* is defined as an arbitrary element in $hgt(D)$, i.e.,

$y^* = any\ point\ in\ hgt(D)$. The mean of maximum defuzzifier is defined as:

$$y^* = \frac{\int_{hgt} y\mu_D(y)dy}{\int_{hgt} \mu_D(y)dy}$$ (3.10)

where $\int_{hgt}(D)$ is an integration for the continuous part of $hgt(D)$ and it is a summation for the discrete part of $hgt(D)$.

3.4 Fuzzy Rule Bases

The fuzzy rule base consists of fuzzy **IF-THEN** rules. It is the core of the fuzzy system in a sense. And all other stages are used to implement these rules in a reasonable and efficient manner. Hence, the fuzzy rule base comprises the following fuzzy **IF-THEN** rules:

Rule i: **IF** x_l is A_1^i and ...and x_n is A_n^i **THEN** y is D^i (3.11)

The canonical fuzzy **IF-THEN** rules in the form of (3.11) includes the following

ones:

(1) Partial rules:

  IF x_1 is A_1^i and …and x_m is A_m^i **THEN** y is D^i　　　　　　　　(3.12)

(2) Or rules

  IF x_1 is A_1^i and …and x_m is A_m^i or x_{m+1} is A_{m+1}^i and … x_n is A_n^i **THEN** y is

  D^i　　　　　　　　(3.13)

(3) Singles fuzzy statement

    y is D^i　　　　　　　　(3.14)

3.5 Fuzzy Inference

  The fuzzy inference is a reasoning method using the fuzzy theory, and whereby the

expert knowledge is presented using linguistic rules. The fuzzy inference introduced

as following.

Product Inference: $\mu_D(y) = \max_{l=1}^{M}[\sup_{x \in U}(\mu_A(x)\prod \mu_{A_i^l}(x_i)\mu_D(y))]$　　　　　　(3.15)

Minimum Inference: $\mu_D(y) = \max_{l=1}^{M}[\sup_{x \in U} \min(\mu_A(x), \mu_{A_1^l}(x_1)..., \mu_{A_n^l}(x_n), \mu_{D^l}(y))]$　　　(3.16)

The product inference and minimum inference are the most commonly used fuzzy

inference in the fuzzy system and other fuzzy applications. In the Fig.3-2 shows the

product inference and minimum inference [25-26].
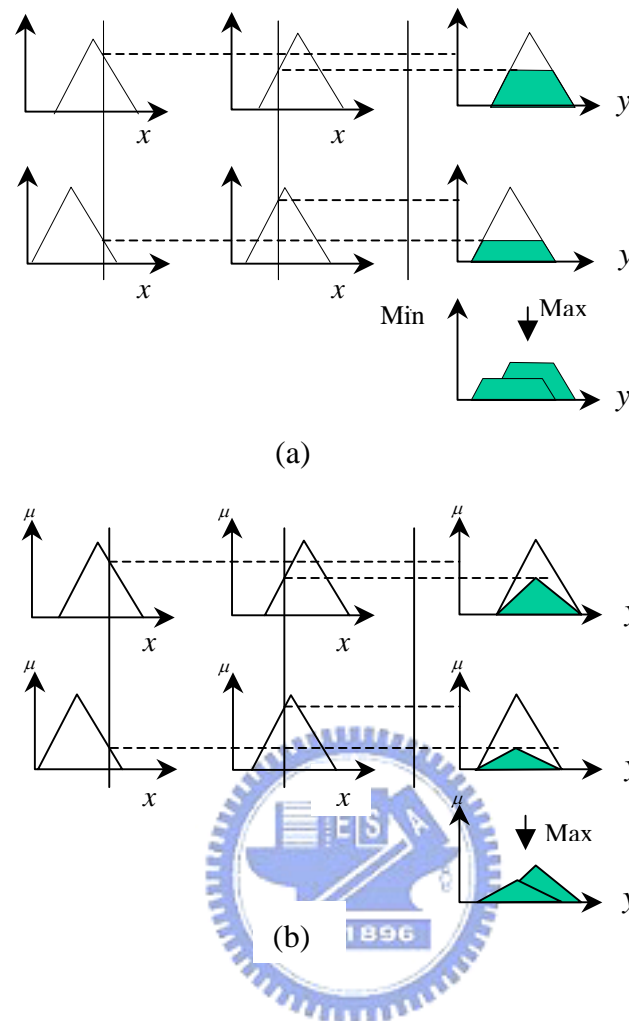
Fig. 3-2 (a) Minimum inference (b) Product inference

3.6 Longitudinal Fuzzy Logic Control of a Platoon of Vehicles

In this section, we design a FLC by imitating a PD controller [6] for a platoon

of vehicles. Design procedures are stated below.

Step 1) Define Δ_i and $\dot{\Delta}_i$ from Eq.(2.1) as two input variables of ith FLC; and

u_i as an output variable of ith FLC; the membership functions for input $\Delta_i, \dot{\Delta}_i$ and

output u_i are shown in Fig. 3-3.
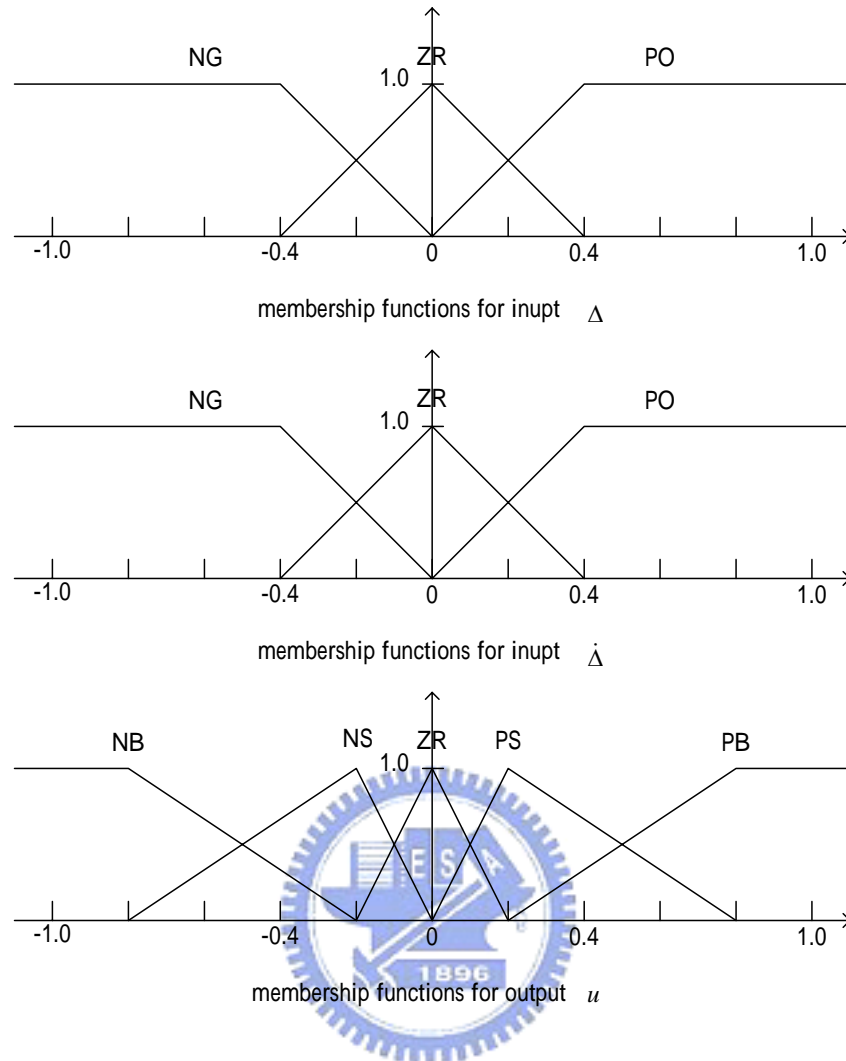
Fig. 3-3 Membership function for input and output variables

Step 2) The main idea is : " if $\Delta_i > 0$, input positive net force to decrease the space of two vehicles; if $\Delta_i < 0$, input negative net force to increase the space of two vehicles; $\dot{\Delta}_i$ is used to amend the strategy above" Table. 3-1 is the rule base we obtain.

Step 3) Select one type of the fuzzifiers, defuzzifiers, and fuzzy inferences. The most frequently used triangular membership, the center-of-gravity defuzzification, and the "max-min" reasoning method are adopted here to carry out the algorithm.

18

$\dot{\Delta}$ \ Δ	NG	ZR	PO
NG	NB	NS	ZR
ZR	NS	ZR	PS
PO	ZR	PS	PB

Table. 3-1 Rule Base of the Fuzzy Logic Controller

3.7 Simulation Results

To examine the behavior of a platoon of vehicles under the above controller, we run simulations for a platoon consisting of 3 different types of vehicles. Three types of vehicles with their relevant parameters referring to [7][8] are shown in the Table. 3-2 and used in the simulations. In the simulation conducted, all the vehicles are assumed to be initially traveling at the steady-state velocity of $v_0 = 17.9$ m/s (i.e., 40 mph). Beginning at time $t = 0$ s, the lead vehicle's velocity is increased from its steady-state velocity value of 17.9 m/s until it reaches its final value of 21.9 m/s (i.e., 50 mph): the maximum jerk and the peak acceleration values corresponding to this velocity time profile are 0.5 m/s^3 and 1m/s^2, respectively (see Fig. 3-4 and Fig. 3-5). Take three following vehicles as a simulation example, the order of vehicles in the

19

platoon followed the lead vehicle is as follows: Daihatsu Charade CLS followed by

Buick Regal Custom followed by BMW 750iL. Consider the vehicle loading, total

mass of each following vehicle is conditioned by adding vehicle curb mass and

passengers' mass. Fig. 3-6 ~ Fig. 3-9 show the simulation results   :

Type	Daihatsu Charade CLS	Buick Regal Custom	BMW 750iL
Vehicle i	1	2	3
Curb mass(kg)	916	1464	1925
Passengers' mass(kg)	91, 91, 91	64, 64	75
Vehicle mass m_i(kg)	1189	1592	2000
K_{di}(kg/m)	0.44	0.49	0.51
$\tau_i(s)$	0.2	0.25	0.2
k_{mi}(N)	352	392	408

Table. 3-2 Simulation Model Parameters of Fuzzy Logic Control

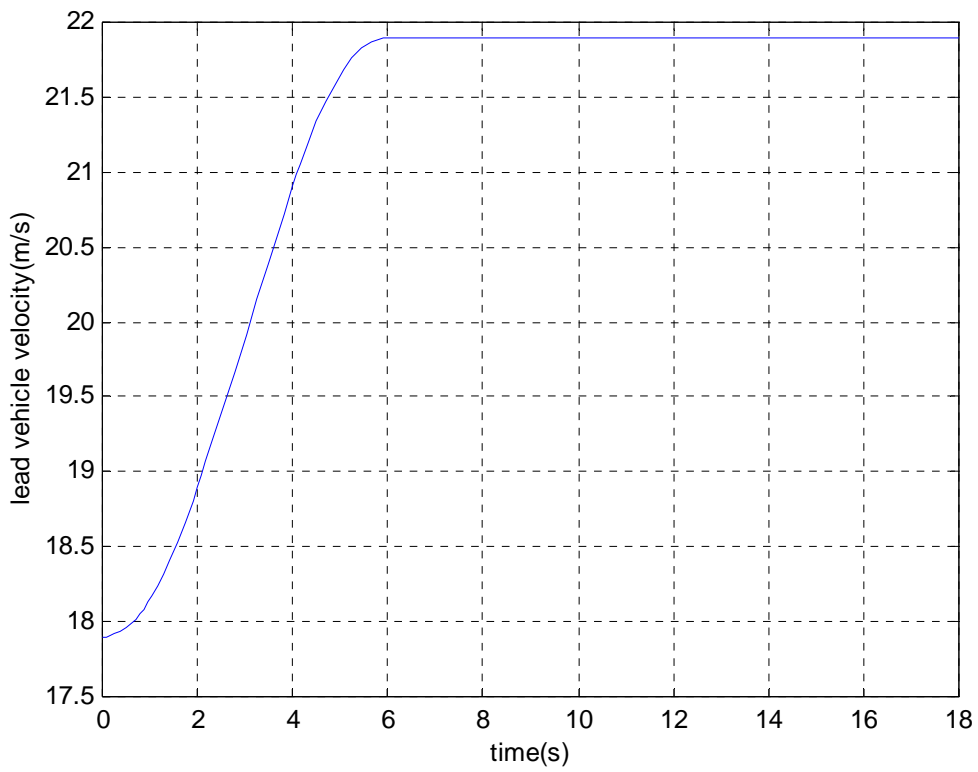**Fig. 3-4 Lead Vehicle's velocity time profile: v_l versus t**
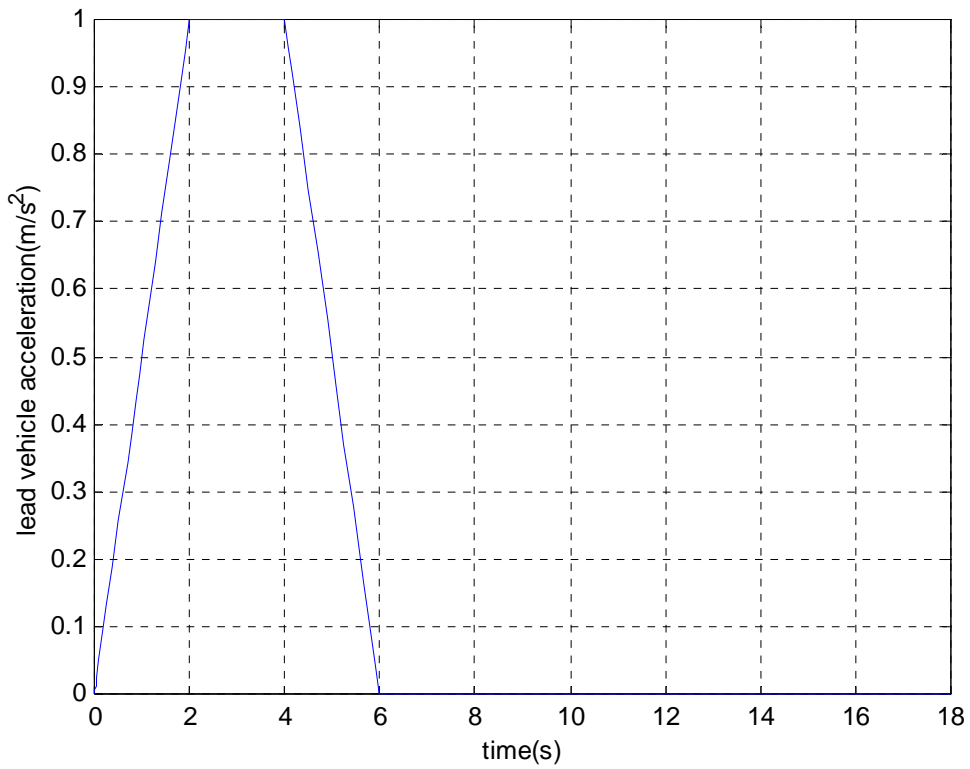
Fig. 3-5 Lead Vehicle's acceleration time profile: a_l versus t
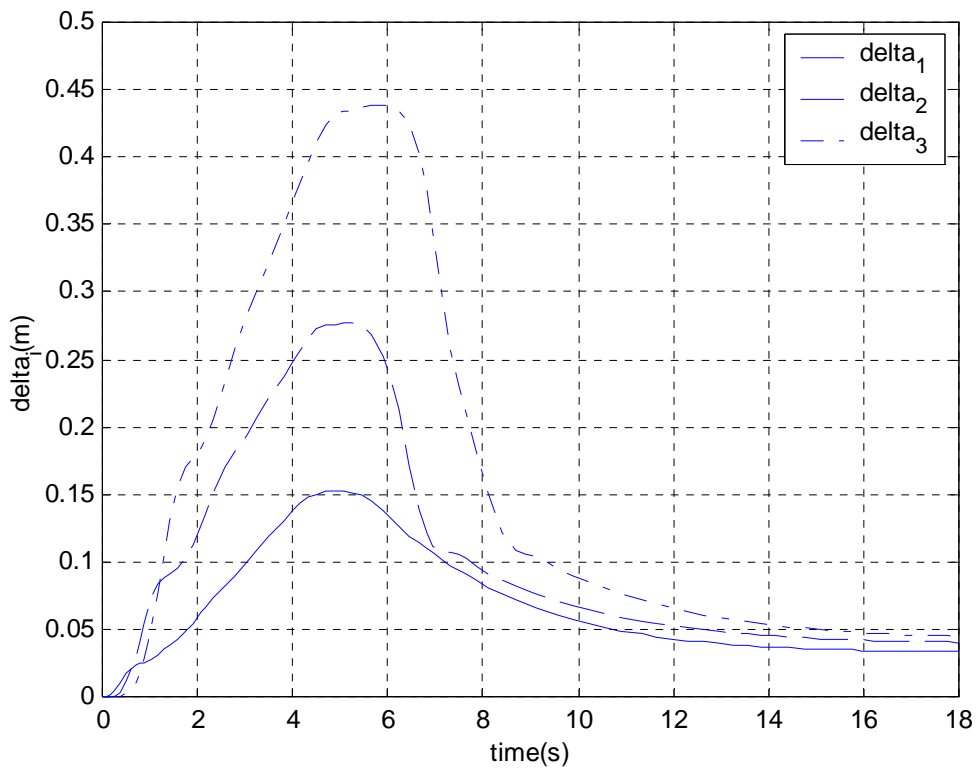
Fig. 3-6 $\Delta_1, \Delta_2, and \Delta_3$ **versus** t
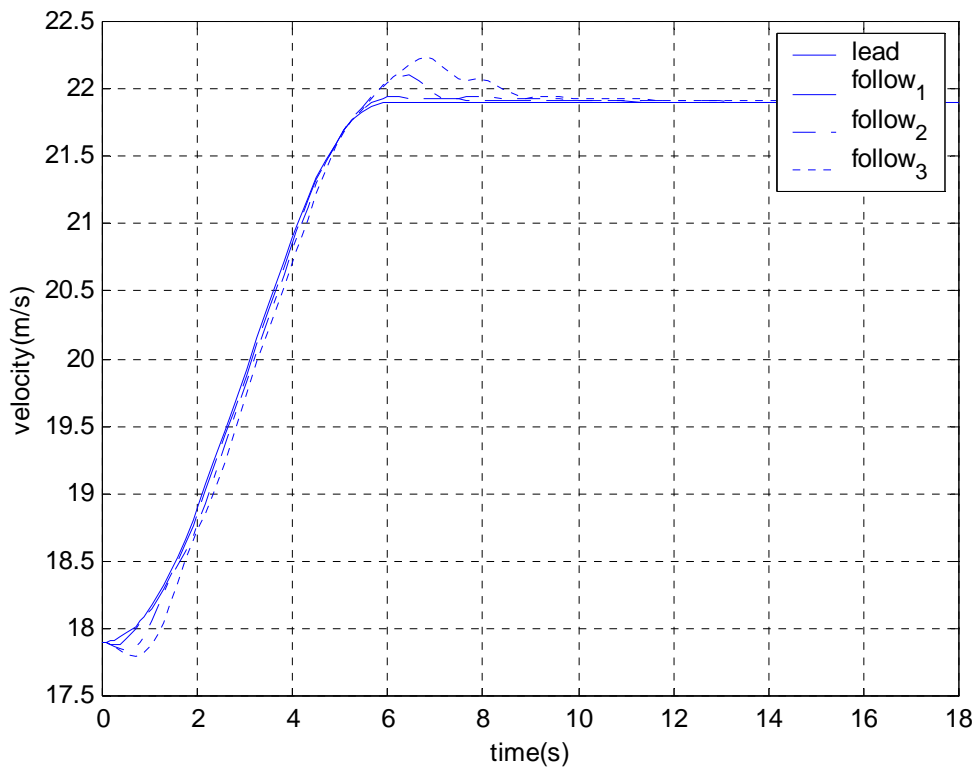
Fig. 3-7 $v_l, v_1, v_2, and v_3$ **versus** t

22
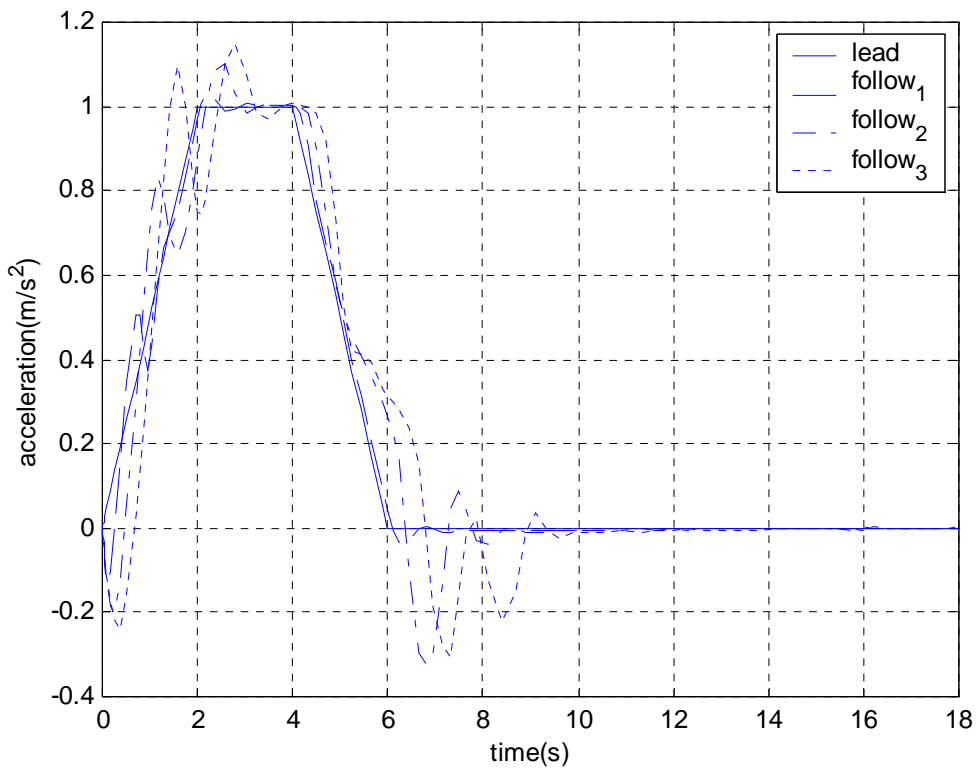
Fig. 3-8 $a_l, a_1, a_2, and\ a_3$ **versus** t

Fig. 3-9 $u_1, u_2, and\ u_3$ **versus** t

23
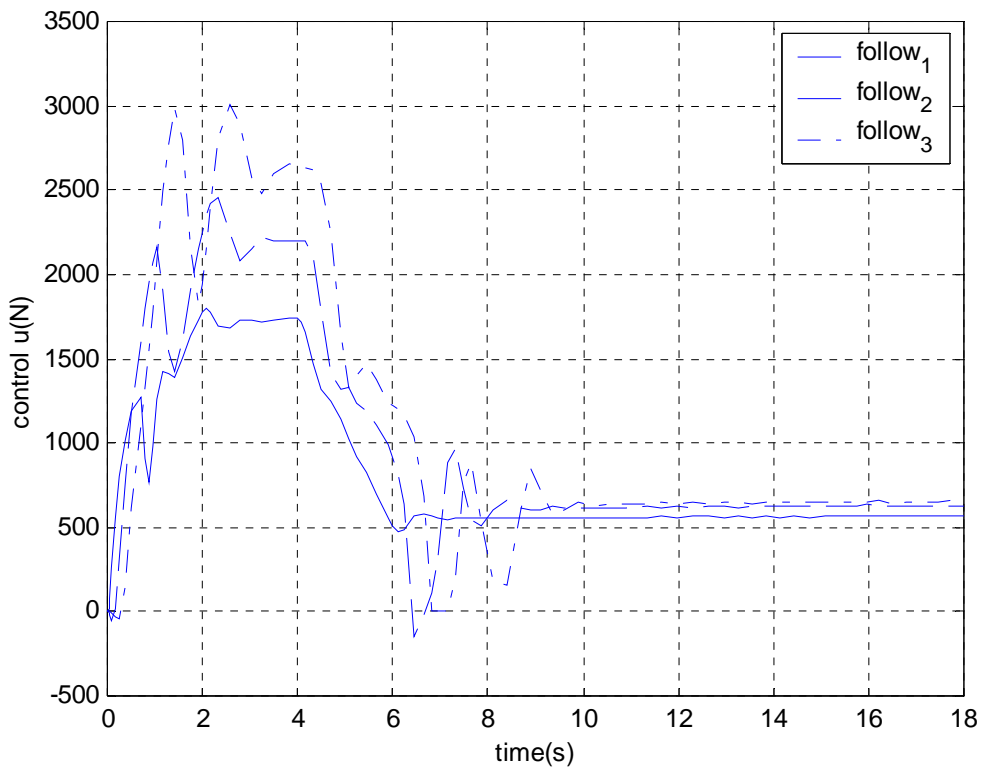
Chapter 4 H∞ Observer-based Sliding Mode Control

with Adaptive Fuzzy Neural Approach

4.1 Fundamental Conceptions of Sliding Control

Model imprecision, which is a common trouble in system control, can have

strong adverse effects on nonlinear control systems. Therefore, any practical design

must address it explicitly. A simple approach to robust control is the so-called sliding

mode control (SMC) methodology. It allows an nth-order problem to be replaced by an

equivalent 1st-order problem, which is intuitively easier to be addressed. For the class

of systems to which it applies, sliding controller design provides a systematic

approach to the problem of maintaining stability and consistent performance in the

face of modeling imprecision.

Take a single-input dynamic system for example:

$$x^{(n)} = f(\mathbf{x}) + b(\mathbf{x})u \tag{4.1}$$

where the scalar x is the output of interest, the scalar u is the control input, and

$\mathbf{x} = [x \quad \dot{x} \quad \cdots \quad x^{(n-1)}]^T$ is the state vector. In equation (4.1), $f(\mathbf{x})$ (in general

nonlinear) is not exactly known, but the extent of the imprecision on $f(\mathbf{x})$ is upper

bounded by a known continuous function of $\mathbf{x}$; similarly, the control gain $b(\mathbf{x})$ is

not exactly known, but is of known sign and bounded by a known, continuous

function of $\mathbf{x}$. The control problem is to get the state $\mathbf{x}$ to track a specific

time-varying state $\mathbf{x}_d = [x_d \quad \dot{x}_d \quad \cdots \quad x_d^{(n-1)}]^T$ in the presence of model impression

on $f(\mathbf{x})$ and $b(\mathbf{x})$.

Let $\tilde{x} = x - x_d$ be the tracking error, and let

$$\tilde{\mathbf{x}} = \mathbf{x} - \mathbf{x}_d = [\tilde{x} \quad \dot{\tilde{x}} \quad \cdots \quad \tilde{x}^{(n-1)}]^T \qquad (4.2)$$

be the tracking error vector. Furthermore, let us define a time-varying surface $s(t)$ in

the state-space $\mathbf{R}^n$ by the scalar equation $s(\mathbf{x};t) = 0$, where

$$s(\mathbf{x};t) = \left(\frac{d}{dt} + \lambda\right)^{n-1} \tilde{x}, \qquad (4.3)$$

and λ is a strictly positive constant. The problem of tracking $\mathbf{x} \equiv \mathbf{x}_d$ is equivalent

to that of remaining on the surface $s(t)$ for all $t > 0$; indeed $s \equiv 0$ represents a

linear differential equation whose unique solution is $\tilde{\mathbf{x}} \equiv 0$ as $t \to \infty$. Thus, the

problem of tracking the n-dimensional vector $\mathbf{x}_d$, i.e., the original n^{th}-order tracking

problem in $\mathbf{x}$, can be replaced by a 1st-order problem of keeping the scalar quantity

s at zero [11]. This simplified 1st-order problem of keeping s at zero can be

achieved by choosing the control law u such that outside of $s(t)$

$$\frac{1}{2}\frac{d}{dt}s^2 \leq -\eta|s|, \qquad (4.4)$$

where η is a strictly positive constant [11]. Eq. (4.4) is called sliding condition.

Essentially, (4.4) states that the squared "distance" to the surface, as measured by s^2,

decreases along all system trajectories.

However, in order to account for the presence of modeling imprecision and disturbances, the control has to be discontinuous across $s(t)$. Since the implementation of the associated control switching is necessarily imperfect, this leads to chattering.

In general, chattering must be eliminated for the controller to perform properly. This can be achieved by smoothing out the control discontinuity in a thin boundary layer neighboring the switching surface

$$\boldsymbol{B}(t) = \{\mathbf{x}, | s(\mathbf{x};t) | \leq \varphi \} \quad \varphi > 0, \tag{4.5}$$

where ϕ is a boundary layer thickness, and $\varepsilon = \phi / \lambda^{n-1}$ is the boundary layer width, as Fig. 4-1 illustrates for the case $n = 2$. In other words, outside $B(t)$, we choose
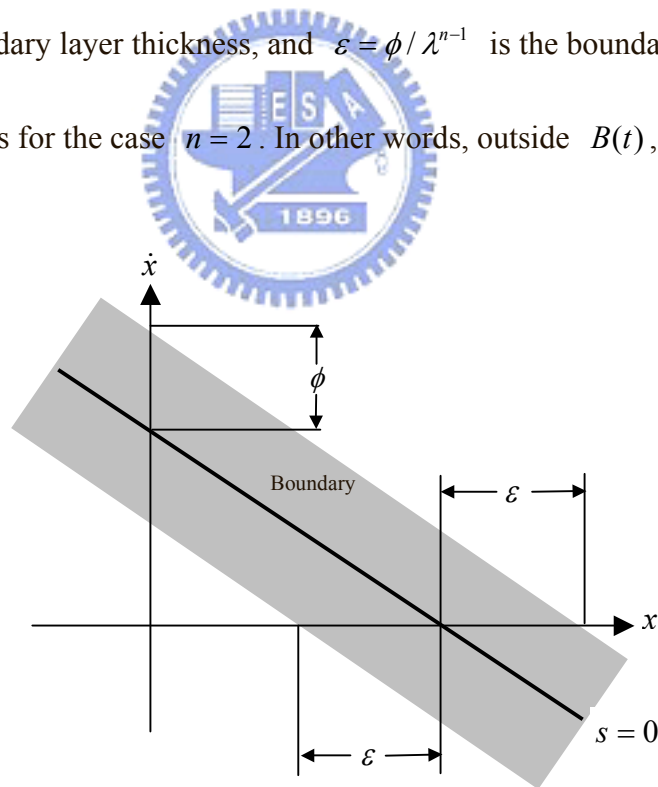
Fig. 4-1 Boundary layer
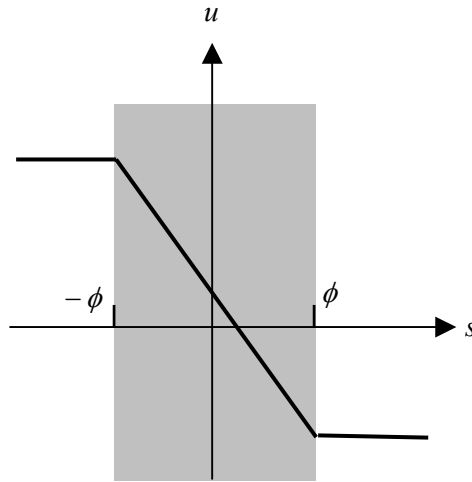
Fig. 4-2 Control interpolation in boundary layer

control u satisfying sliding condition (4.4), which guarantees that the boundary layer

is attractive - hence invariant: all trajectories starting inside $B(t=0)$ remain inside $B(t)$

for all $t \geq 0$. Then, we interpolate u inside $B(t)$, as illustrated in Fig. 4-2. This leads to

tracking within a guaranteed precision ε (rather than "perfect" tracking), and in the

meantime eliminates the chattering.

4.2 Sliding Mode Control

Let's consider the first two vehicles in the forefront of the platoon. We will

discuss the first couple of vehicles for detail thereinafter since the behavior of other

couples of vehicles are similar. By rearranging (2.7) the first follow vehicle dynamic

is written as

$$\begin{cases} \dot{p}_1 = v_1 \\ \dot{v}_1 = a_1 \\ \dot{a}_1 = f_1(v_1, a_1) + g_1(v_1)u_1 \end{cases} \tag{4.6}$$

where

$$f_1(v_1, a_1) = -\frac{1}{\tau_1(v_1)}\left[a_1 + \frac{K_{d1}}{m_1}v_1^2 + \frac{k_{m1}}{m_1}\right] - \frac{2K_{d1}}{m_1}v_1 a_1 \qquad \text{and}$$

$$g_1(v_1) = \frac{1}{m_1 \tau_1(v_1)}$$

And, the lead vehicle dynamic is stated as

$$\begin{cases} \dot{p}_l = v_l \\ \dot{v}_l = a_l \\ \dot{a}_l = Va(t) \end{cases} \tag{4.7}$$

where $p_l = x_l$, $v_l = \dot{x}_l$, $a_l = \ddot{x}_l$, and Va is the variation of acceleration of the lead vehicle for increasing its velocity from v_0 to v_f in a period of time. Substituting Eq. (4.6) and (4.7) to Eq. (2.1), we have

$$\dddot{\Delta} = Va(t) - f_1(v_1, a_1) - g_1(v_1)u_1 \tag{4.8}$$

where $\Delta_1 = x_l - x_1 - L$. Let $\Delta_1 = e_1(1)$, $\dot{\Delta}_1 = e_1(2)$, and $\ddot{\Delta}_1 = e_1(3)$, (4.8) is rewritten as

$$\begin{cases} \dot{e}_1(1) = e_1(2) \\ \dot{e}_1(2) = e_1(3) \\ \dot{e}_1(3) = Va(t) - f_1(v_1, a_1) - g_1(v_1)u_1 \end{cases} \tag{4.9}$$

where $Va(t) - f_1(v_1, a_1)$ is a nonlinear function which depends on v_1 and a_1, and

u_1 stands for the control input. Let $F_1(v_1, a_1) = Va(t) - f_1(v_1, a_1)$ and

$G_1(v_1) = -g_1(v_1)$. Therefore, (4.8) and (4.9) become

$$\dddot{\Delta}_1 = F_1(v_1, a_1) + G_1(v_1)u_1 \tag{4.10}$$

and

$$\begin{cases} \dot{e}_1(1) = e_1(2) \\ \dot{e}_1(2) = e_1(3) \\ \dot{e}_1(3) = F_1(v_1, a_1) + G_1(v_1)u_1 \end{cases} \tag{4.11}$$

Let $\mathbf{e}_1 = [e_1(1) \ e_1(2) \ e_1(3)]^T$. The control target of this case is to find an appropriate

control law u_1 such that the tracking error $\mathbf{e}_1$ is zero. Furthermore, let the sliding

surface $s(t)$ be expressed in the state-space R^3 by the scalar equation $s(\mathbf{e}_1; t) = 0$

as

$$s(\mathbf{e}_1; t) = \left(\frac{d}{dt} + \lambda \right)^2 e_1(1) = e_1(3) + 2\lambda\, e_1(2) + \lambda^2 e_1(1), \quad \lambda > 0 \tag{4.12}$$

From (4.11), (4.12), and following similar derivations in [5], we can use the sliding

mode control method and obtain a control law derived in *Lemma 1*.

Lemma 1: Consider the nonlinear system (4.11) with given nonlinear function

$F_1(v_1, a_1)$. Suppose that control input is chosen as

$$u_1 = G_1(v_1)^{-1}[-F_1(v_1, a_1) - \lambda^2 e_1(2) - 2\lambda e_1(3) - p_{21}e_1(1) - p_{22}e_1(2) - k\,sign(s(\mathbf{e}_1; t))]$$

$$\tag{4.13}$$

and that $\mathbf{P}$ is positive definite symmetric matrix, $\mathbf{P} \in R^{2 \times 2}$ satisfies the Lyapunov

matrix equation

$$\mathbf{A}_1^T \mathbf{P} + \mathbf{P}\mathbf{A}_1 = -\mathbf{Q} \tag{4.14}$$

where $sign(s(\mathbf{e}_1;t)) = \begin{cases} 1 & if\ s(\mathbf{e}_1;t) > 0 \\ -1 & if\ s(\mathbf{e}_1;t) < 0 \end{cases}$, $\mathbf{A}_1 = \begin{bmatrix} 0 & 1 \\ -\lambda^2 & -2\lambda \end{bmatrix}$ is Hurwitz, p_{21},

p_{22} are elements of $\mathbf{P}$, and $\mathbf{Q} > 0$ is given. Then $s \to 0$ and $\mathbf{e}_1 \to 0$ as $t \to \infty$.

Proof:

From Eq.(4.12), we have $e_1(3) = -\lambda^2 e_1(1) - 2\lambda e_1(2) + s$.

Let $\bar{\mathbf{e}}_1 = [e_1(1) \quad e_1(2)]^T$, then

$$\dot{\bar{\mathbf{e}}}_1 = [e_1(2) \quad e_1(3)]^T = \begin{bmatrix} 0 & 1 \\ -\lambda^2 & -2\lambda \end{bmatrix} \bar{\mathbf{e}}_1 + \begin{bmatrix} 0 \\ s \end{bmatrix} \tag{4.15}$$

Consider a Lyapunov function candidate as following:

$$v = \frac{1}{2}s^2 + \frac{1}{2}\bar{\mathbf{e}}_1{}^T \mathbf{P}\bar{\mathbf{e}}_1 \tag{4.16}$$

here $\mathbf{P}$ is positive definite symmetric matrix.

By using (4.11), (4.12), (4.14), and (4.15), the time derivative of (4.16) is

$$\dot{v} = s\dot{s} + \bar{\mathbf{e}}_1{}^T \mathbf{P}\dot{\bar{\mathbf{e}}}_1 = s[\lambda^2 e_1(2) + 2\lambda e_1(3) + F_1 + G_1 u_1] + \bar{\mathbf{e}}_1{}^T \mathbf{P}(\begin{bmatrix} 0 & 1 \\ -\lambda^2 & -2\lambda \end{bmatrix}\bar{\mathbf{e}}_1 + \begin{bmatrix} 0 \\ s \end{bmatrix})$$

$$= s[\lambda^2 e_1(2) + 2\lambda e_1(3) + F_1 + G_1 u_1] + \bar{\mathbf{e}}_1{}^T \mathbf{P}\mathbf{A}_1\bar{\mathbf{e}}_1 + \bar{\mathbf{e}}_1{}^T \mathbf{P}\begin{bmatrix} 0 \\ s \end{bmatrix}$$

$$= s[\lambda^2 e_1(2) + 2\lambda e_1(3) + F_1 + G_1 u_1] + \frac{1}{2}\bar{\mathbf{e}}_1{}^T [\mathbf{P}\mathbf{A}_1 + \mathbf{A}_1{}^T \mathbf{P}]\bar{\mathbf{e}}_1 + \bar{\mathbf{e}}_1{}^T \mathbf{P}\begin{bmatrix} 0 \\ s \end{bmatrix} \tag{4.17}$$

Apply (4.13) to (4.17), we have the following relationship:

$$\dot{v} = -ks \cdot sign(s) - \frac{1}{2}\bar{\mathbf{e}}_1{}^T \mathbf{Q}\bar{\mathbf{e}}_1 = -k|s| - \frac{1}{2}\bar{\mathbf{e}}_1{}^T \mathbf{Q}\bar{\mathbf{e}}_1 < 0 \quad \forall s \neq 0\ and\ \bar{\mathbf{e}}_1 \neq 0 \tag{4.18}$$

We conclude $s \to 0$ and $\bar{\mathbf{e}}_1 \to 0$ ($\mathbf{e}_1 \to 0$) as $t \to \infty$. This completes the proof.

Note that if we include the design of (4.5), (4.13) becomes

$$u_1 = G_1(v_1)^{-1}[-F_1(v_1, a_1) - \lambda^2 e_1(2) - 2\lambda e_1(3) - p_{21}e_1(1) - p_{22}e_1(2) - ksat(s(\mathbf{e}_1;t)/\phi)]$$

$$; \phi > 0 \quad (4.19)$$

where $sat(s(\mathbf{e}_1;t)/\phi) = \begin{cases} s/\phi & if |s/\phi| \leq 1 \\ sign(s/\phi) & otherwise \end{cases}$,

$$sign(s/\phi) = \begin{cases} 1 & if \ (s/\phi) > 0 \\ -1 & if \ (s/\phi) < 0 \end{cases}.$$

4.3 Sliding Mode Control with Fuzzy Neural Network Approximator

In practical applications, however, $F_1(v_1, a_1)$ is generally uncertain rather than given. The controller of (4.13) derived above is not always obtainable. Therefore, a new controller needs to be designed taking into account the unknown nonlinear function, which will be adequately approximated by a fuzzy-neural approximator.

The configuration of the fuzzy-neural network shown in Fig. 4-3 consists of a fuzzy system and neural network. The fuzzy system can be divided into two parts: some fuzzy IF-THEN rules and a fuzzy inference engine. The fuzzy inference engine uses the fuzzy IF-THEN rules to perform a mapping from an input linguistic vector $\mathbf{e}_1 = [e_1(1) \quad e_1(2) \quad e_1(3)]^T \in \mathbf{R}^3$ to an output linguistic variable $o(\mathbf{e}_1) \in \mathbf{R}$.

The ith fuzzy IF-THEN rule is written as

$\mathbf{R}^i$: If $e_1(1)$ is A_1^i and $e_1(2)$ is A_2^i and $e_1(3)$ is A_3^i than y^i is B^i (4.20)

where A_1^i, A_2^i, A_3^i and B^i are fuzzy sets with membership functions $\mu_{A_j^i}(e_1(j))$ and $\mu_{B^i}(y^i)$. And y^i is the point at which $\mu_{B^i}(y^i) = 1$. By using produce inference, center-average and singleton fuzzifier, the output of the fuzzy-neural network can be

expressed as
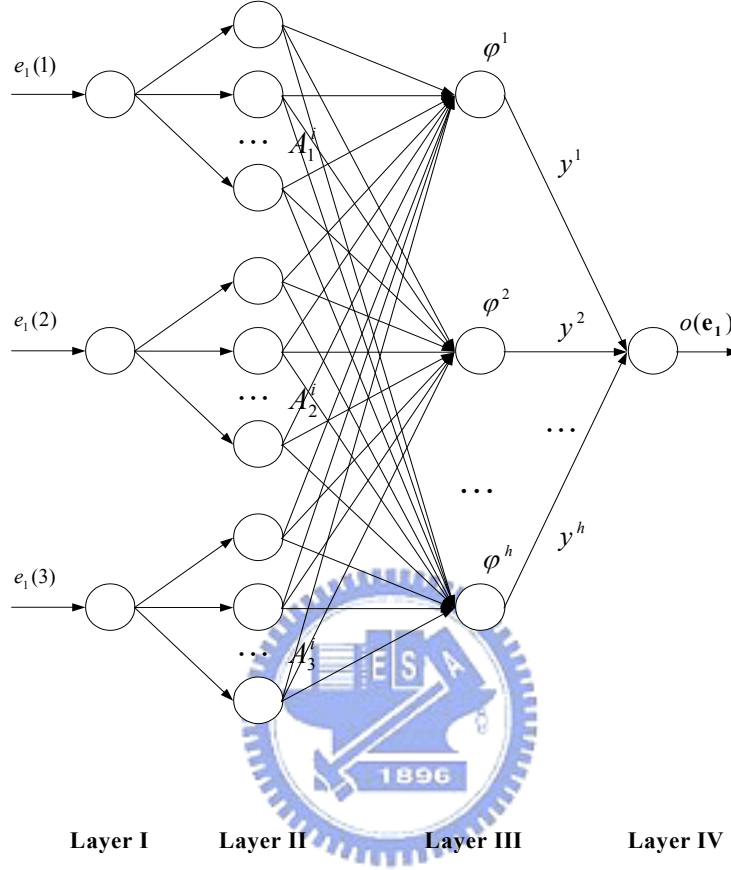
Fig. 4-3 Configuration of a fuzzy-neural approximator

$$o(\mathbf{e_1}) = \frac{\sum\limits_{i=1}^{h} y^i \left[\prod\limits_{j=1}^{3} \mu_{A_j^i}(e_1(j)) \right]}{\sum\limits_{i=1}^{h} \left[\prod\limits_{j=1}^{3} \mu_{A_j^i}(e_1(j)) \right]} \tag{4.21}$$

$$= \boldsymbol{\theta}^T \varphi(\mathbf{e_1})$$

where $\mu_{A_j^i}(e_1(j))$ is the membership function value of the fuzzy variable $e_1(j)$,

h is the total number of the IF-THEN rules , y^i is the point at which $\mu_{B^i}(y^i) = 1$,

$\boldsymbol{\theta} = [y^1 \quad y^2 \quad \cdots \quad y^h]^T$ is an adjustable parameter vector, and

$\varphi = [\varphi^1 \quad \varphi^2 \quad \cdots \quad \varphi^h]^T$ is a fuzzy basis vector, where φ^i is defined as

$$\varphi^i(\mathbf{e_1}) = \frac{\prod\limits_{j=1}^{3} \mu_{A_j^i}(e_1(j))}{\sum\limits_{i=1}^{h}\left[\prod\limits_{j=1}^{3} \mu_{A_j^i}(e_1(j))\right]} \ . \tag{4.22}$$

When the inputs are given into the fuzzy-neural network shown in Fig. 4-3, the truth value φ^i (layer III) of the antecedent part of the ith implication is calculated by (4.22). Among the commonly used defuzzification strategies, the output (layer IV) of the fuzzy-neural network is expressed as (4.21). Therefore, the fuzzy logic approximator based on the neural network can be established. Fig. 4-3 shows the configuration of the fuzzy-neural function approximator. The approximator has four layers. At layer I, input nodes stand for the input linguistic variables $e_1(1)$, $e_1(2)$, and $e_1(3)$. At layer II, nodes represent the values of the membership functions. At layer III, nodes are the values of the fuzzy basis vector φ. Each node of layer III performs a fuzzy rule. The links between layer III and layer IV are full connected by the weighting factors $\mathbf{\theta} = [y^1 \quad y^2 \quad \cdots \quad y^h]^T$, i.e., the adjusted parameters. At layer IV, the output stands for the value of $o(\mathbf{e_1})$.

To approximate the uncertain nonlinear function $F_1(v_1, a_1)$ in (4.11), adaptive update laws to adjust the parameter vector $\mathbf{\theta}$ in (4.21) of the fuzzy-neural approximator need to be developed. Let $\hat{F}_1$ be the estimation function for the uncertain nonlinear function F_1. That is,

$$\hat{F}_1(\mathbf{e_1} \mid \mathbf{\theta}) = \mathbf{\theta}^T \varphi(\mathbf{e_1}) \tag{4.23}$$

33

In order to derive the adaptive update law, the following assumption is required.

Assumption 1 [27]:

Let $\mathbf{e_1}$ belongs to a compact set $U_{\mathbf{e_1}} = \{\ \mathbf{e_1} \in \mathbf{R}^3 : \|\mathbf{e_1}\| \le m_{\mathbf{e_1}} < \infty\ \}$ and $m_{\mathbf{e}}$ is

designed parameter. It is known a prior that the optimal parameter vector

$\theta^* = \arg\min\limits_{\theta \in M_\theta}[\ \sup\limits_{\mathbf{e_1} \in U_{\mathbf{e_1}}} |F_1 - \hat{F}_1(\mathbf{e_1} \mid \theta)|]$ lies   in   some   convex   region

$M_\theta = \{\ \theta \in \mathbf{R}^3 : \|\theta\| \le m_\theta\ \}$, where the radius m_θ is constant.

Thus, to approximate the uncertain nonlinear term F_1, Eq. (4.10) becomes

$$\dddot{\Delta}_1 = \theta^{*T}\varphi(\mathbf{e_1}) + G_1(v_1)u_1 + w \tag{4.24}$$

where $w = F_1 - \theta^{*T}\varphi(\mathbf{e_1})$ is the lumped uncertainty.

To facilitate the design process of the controller, the lumped uncertainty is generally

assumed to have an upper bound,

$$|w| \le w^u, \quad w^u \text{ is a positive constant} \tag{4.25}$$

Based on above condition, a control law via fuzzy-neural approximator can be

obtained from *Lemma 2* below.

Lemma 2: Consider the nonlinear system (4.11) with uncertain nonlinear function

$F_1(v_1, a_1)$, which is approximated as (4.24). Suppose *Assumption 1* and (4.25) are

satisfied and control input is chosen as

$$u_1 = G_1(v_1)^{-1}[-\hat{\boldsymbol{\theta}}^T \varphi(\mathbf{e_1}) - \lambda^2 e_1(2) - 2\lambda e_1(3) - p_{21}e_1(1) - p_{22}e_1(2) - k\, sign(s(\mathbf{e_1};t))]$$

<div align="right">(4.26)</div>

where $\hat{\boldsymbol{\theta}}$ is the estimate of $\boldsymbol{\theta}^*$, and the update law is chosen as

$$\dot{\hat{\boldsymbol{\theta}}} = \Gamma s \varphi$$

<div align="right">(4.27)</div>

where $\Gamma > 0$ is the adaptation matrix, $k = k_2 + w^u$, $k_2 > 0$, and s is the sliding surface.

Then $s \to 0$ and $\mathbf{e_1} \to 0$ as $t \to \infty$.

Proof:

Consider the Lyapunov function

$$v = \frac{1}{2}s^2 + \frac{1}{2}\bar{\mathbf{e}}_1{}^T \mathbf{P}\bar{\mathbf{e}}_1 + \frac{1}{2}\tilde{\boldsymbol{\theta}}^T \boldsymbol{\Gamma}^{-1}\tilde{\boldsymbol{\theta}}$$

<div align="right">(4.28)</div>

where $\tilde{\boldsymbol{\theta}} = \boldsymbol{\theta}^* - \hat{\boldsymbol{\theta}}$.

The time derivative of (4.28) is

$$\dot{v} = s\dot{s} + \frac{1}{2}\bar{\mathbf{e}}_1{}^T \mathbf{P}\dot{\bar{\mathbf{e}}}_1 + \frac{1}{2}\dot{\bar{\mathbf{e}}}_1{}^T \mathbf{P}\bar{\mathbf{e}}_1 + \frac{1}{2}\tilde{\boldsymbol{\theta}}^T \boldsymbol{\Gamma}^{-1}\dot{\tilde{\boldsymbol{\theta}}} + \frac{1}{2}\dot{\tilde{\boldsymbol{\theta}}}^T \boldsymbol{\Gamma}^{-1}\tilde{\boldsymbol{\theta}}$$

$$= s[\lambda^2 \dot{e}_1(1) + 2\lambda\dot{e}_1(2) + \dot{e}_1(3)] + \bar{\mathbf{e}}_1{}^T \mathbf{P}(\mathbf{A_1}\bar{\mathbf{e}}_1 + [0\ s]^T) + \tilde{\boldsymbol{\theta}}^T \boldsymbol{\Gamma}^{-1}(-\dot{\hat{\boldsymbol{\theta}}})$$

$$= s[\lambda^2 e_1(2) + 2\lambda e_1(3) + \boldsymbol{\theta}^{*T}\varphi(\mathbf{e_1}) + G_1(v_1)u_1 + w] + \frac{1}{2}\bar{\mathbf{e}}_1{}^T(\mathbf{PA_1} + \mathbf{A_1}{}^T\mathbf{P})\bar{\mathbf{e}}_1 + \bar{\mathbf{e}}_1{}^T\mathbf{P}[0\ s]^T + \tilde{\boldsymbol{\theta}}^T\boldsymbol{\Gamma}^{-1}(-\dot{\hat{\boldsymbol{\theta}}})$$

$$= s[\lambda^2 e_1(2) + 2\lambda e_1(3) + \boldsymbol{\theta}^{*T}\varphi(\mathbf{e_1}) + G_1(v_1)u_1 + w] - \frac{1}{2}\bar{\mathbf{e}}_1{}^T\mathbf{Q}\bar{\mathbf{e}}_1\dot{\hat{\boldsymbol{\theta}}}$$

$$+ s(e_1(1)p_{12} + e_1(2)p_{22}) - \tilde{\boldsymbol{\theta}}^T\boldsymbol{\Gamma}^{-1}\dot{\hat{\boldsymbol{\theta}}}$$

<div align="right">(4.29)</div>

Apply (4.26) and (4.27) to (4.29), and let $k = k_2 + w^u$, we have following relationship:

$$\dot{v} = s[\tilde{\boldsymbol{\theta}}^T \varphi(\mathbf{e_1}) - p_{21}e_1(1) - p_{22}e_1(2) - k\ sign(s(\mathbf{e_1};t)) + w] - \frac{1}{2}\bar{\mathbf{e}}_1^{\ T}\mathbf{Q}\bar{\mathbf{e}}_1 + s(e_1(1)p_{21} + e_1(2)p_{22}) - \tilde{\boldsymbol{\theta}}^T\boldsymbol{\Gamma}^{-1}\dot{\hat{\boldsymbol{\theta}}}$$

$$= s[\tilde{\boldsymbol{\theta}}^T \varphi(\mathbf{e_1}) - k\ sign(s(\mathbf{e_1};t)) + w] - \frac{1}{2}\bar{\mathbf{e}}_1^{\ T}\mathbf{Q}\bar{\mathbf{e}}_1 - \tilde{\boldsymbol{\theta}}^T\boldsymbol{\Gamma}^{-1}(\boldsymbol{\Gamma}s\varphi(\mathbf{e_1}))$$

$$= s[-(k_2 + w^u)sign\ (s) + w] - \frac{1}{2}\bar{\mathbf{e}}_1^{\ T}\mathbf{Q}\,\bar{\mathbf{e}}_1$$

$$< -k_2|s| - \frac{1}{2}\bar{\mathbf{e}}_1^{\ T}\mathbf{Q}\bar{\mathbf{e}}_1 < 0 \qquad \forall s \neq 0 \text{ and } \bar{\mathbf{e}}_1 \neq 0 \tag{4.30}$$

We conclude $s \to 0$ and $\mathbf{e_1} \to 0$ as $t \to \infty$. This completes the proof.

4.4 Sliding Mode Control with Fuzzy Neural Network Approximator and $\mathbf{H}_\infty$ performance

As shown in (4.25) and (4.26), $k = k_2 + w^u$ needs to be determined in advance to construct the control input u_1, In practical applications, however, the exact upper bound w^u cannot be chosen so as to attenuate the uncertainties, large control chattering nevertheless occurs. Simulation with a sliding mode controller illustrate this effects for different k selected. To relax the impractical constraint, a new control law is designed by using the H_∞ tracking design technique based on a much relaxed assumption [5], The lumped uncertainty is assumed such that

$$w \in L_2[0,T], \forall T \in [0,\infty) \tag{4.31}$$

Lemma 3:

Consider the nonlinear system (4.11) with uncertain nonlinear function $F_1(v_1, a_1)$, which is approximated as (4.24). Suppose *Assumption 1*, Eq. (4.25), and Eq. (4.31)

are satisfied; the control input is chosen as

$$u_1 = G_1(v_1)^{-1}[-\hat{\boldsymbol{\theta}}^T \varphi(\mathbf{e_1}) - \lambda^2 e_1(2) - 2\lambda e_1(3) - p_{21}e_1(1) - p_{22}e_1(2) - \frac{s}{2\rho^2}]$$

(4.32)

and the update law as (4.27), where $\rho > 0$ is the design constant serving as an attenuation level, s is the sliding surface. Then the H_∞ tracking performance [9], [10] for the overall system satisfies the following relationship:

$$\frac{1}{2}\int_0^T \mathbf{\bar{e}_1}^T \mathbf{Q}\mathbf{\bar{e}_1} d\tau \leq \frac{1}{2}s^2(0) + \frac{1}{2}\mathbf{\bar{e}_1}^T(0)\mathbf{P}\mathbf{\bar{e}_1}(0) + \frac{1}{2}\widetilde{\boldsymbol{\theta}}^T(0)\Gamma^{-1}\widetilde{\boldsymbol{\theta}}(0) + \frac{1}{2}\rho^2\int_0^T w^2(\tau)d\tau$$

(4.33)

where $\widetilde{\boldsymbol{\theta}} = \boldsymbol{\theta}^* - \hat{\boldsymbol{\theta}}$.

Proof:

Consider the Lyapunov function

$$v = \frac{1}{2}s^2 + \frac{1}{2}\mathbf{\bar{e}_1}^T \mathbf{P}\mathbf{\bar{e}_1} + \frac{1}{2}\widetilde{\boldsymbol{\theta}}^T \Gamma^{-1}\widetilde{\boldsymbol{\theta}}$$

(4.34)

The time derivative of (4.34) is (see (4.29))

$$\dot{v} = s[\lambda^2 e_1(2) + 2\lambda e_1(3) + \boldsymbol{\theta}^{*T}\varphi(\mathbf{e_1}) + G_1(v_1)u_1 + w] - \frac{1}{2}\mathbf{\bar{e}_1}^T \mathbf{Q}\mathbf{\bar{e}_1} + s(e_1(1)p_{12} + e_1(2)p_{22}) - \widetilde{\boldsymbol{\theta}}^T \Gamma^{-1}\dot{\hat{\boldsymbol{\theta}}}$$

(4.35)

Apply (4.27) and (4.32) to (4.35), we have

$$\dot{v} = \frac{-1}{2}\mathbf{\bar{e}_1}^T \mathbf{Q}\mathbf{\bar{e}_1} - \frac{1}{2}(\frac{s}{\rho} - \rho w)^2 + \frac{1}{2}\rho^2 w^2 \leq \frac{-1}{2}\mathbf{\bar{e}_1}^T \mathbf{Q}\mathbf{\bar{e}_1} + \frac{1}{2}\rho^2 w^2$$

(4.36)

By (4.31), we integrate (4.36) from $t=0$ to $t=T$, and obtain

37

$$\frac{1}{2}\int_0^T \bar{\mathbf{e}}_\mathbf{1}^{\ T}(\tau)\mathbf{Q}\bar{\mathbf{e}}_\mathbf{1}(\tau)d\tau \le v(0) + \frac{1}{2}\rho^2\int_0^T w^2(\tau)d\tau \tag{4.37}$$

Substituting (4.34) to (4.37), we have the H_∞ tracking performance, satisfying (4.33)

$$\frac{1}{2}\int_0^T \bar{\mathbf{e}}_\mathbf{1}^{\ T}\mathbf{Q}\bar{\mathbf{e}}_\mathbf{1}d\tau \le \frac{1}{2}s^2(0) + \frac{1}{2}\bar{\mathbf{e}}_\mathbf{1}^{\ T}(0)\mathbf{P}\bar{\mathbf{e}}_\mathbf{1}(0) + \frac{1}{2}\tilde{\boldsymbol{\theta}}^T(0)\boldsymbol{\Gamma}^{-1}\tilde{\boldsymbol{\theta}}(0) + \frac{1}{2}\rho^2\int_0^T w^2(\tau)d\tau$$

This completes the proof.

Remark:

If a set of initial condition $\bar{\mathbf{e}}_\mathbf{1}(0) = 0$, $s(0) = 0$, $\hat{\boldsymbol{\theta}}(0) = \boldsymbol{\theta}^*(0)$ can be obtained, and **Q=I**, then control performance of the overall system satisfies

$$\sup_{w\in L_2}\frac{\|\bar{\mathbf{e}}_\mathbf{1}\|_2}{\|w\|_2} \le \rho \tag{4.38}$$

where $\|\bar{\mathbf{e}}_\mathbf{1}\|_2^2 = \int_0^T \bar{\mathbf{e}}_\mathbf{1}^{\ T}(\tau)\bar{\mathbf{e}}_\mathbf{1}(\tau)d\tau$, $\|w\|_2^2 = \int_0^T w^2(\tau)d\tau$. That is, an arbitrary attenuation level can be obtained, if ρ is adequately chosen.

4.5 Observer-based Sliding Mode Control with Fuzzy Neural Network Approximator and H_∞ performance

Utilizing sensors to obtain the measurements of the parameters in the vehicle system, such as the velocity, the acceleration,… etc., is difficult or expensive. Considering the technical difficulties and the economic benefits, we adopt an observer to estimate the plant output state vector while we assume that only the headway information of two vehicles is measurable. Under this constraint, a sliding mode

observer is proposed for state estimation [3][37]. The sliding observers offer

advantages similar to those of sliding controllers such as robustness to parameter

uncertainty and easy application to important classes of nonlinear systems.

In this section, our task is to combine the plant and controller with an sliding

observer which estimates the state vector $\mathbf{e_1}$; the estimated vector is denoted as $\hat{\mathbf{e}}_1$

and used as the input both of the sliding mode controller and of the adaptive

fuzzy-neural network approximator   instead of state feedback $\mathbf{e_1}$ used before.

Rewrite (4.11) as

$$\begin{cases} \dot{e}_1(1) = e_1(2) \\ \dot{e}_1(2) = e_1(3) \\ \dot{e}_1(3) = H_1(\mathbf{e_1}, u_1) \end{cases} \tag{4.39}$$

where $H_1(\mathbf{e_1}, u_1) = F_1 + G_1 u_1$.

Consider the following observer [3][37][32]:

$$\begin{cases} \dot{\hat{e}}_1(1) = \hat{e}_1(2) + \lambda_1 \, sign(e_1(1) - \hat{e}_1(1)) \\ \dot{\hat{e}}_1(2) = \hat{e}_1(3) + \lambda_2 \, sign(e_1(1) - \hat{e}_1(1)) \\ \dot{\hat{e}}_1(3) = H_1(\hat{\mathbf{e}}_1, u_1) + \lambda_3 \, sign(e_1(1) - \hat{e}_1(1)) \end{cases} \tag{4.40}$$

where $\hat{\mathbf{e}}_1 = [\hat{e}_1(1) \; \hat{e}_1(2) \; \hat{e}_1(3)]^T$ are the observer output states; $\mathbf{P^o}$ is positive definite

symmetric matrix, $\mathbf{P^o} \in R^{2x2}$ satisfies the Lyapunov matrix equation

$$\mathbf{A}^{o^T}\mathbf{P^o} + \mathbf{P^o}\mathbf{A^o} = -\mathbf{I} \tag{4.41}$$

where $\mathbf{A^o} = \begin{bmatrix} -\dfrac{\lambda_2}{\lambda_1} & 1 \\ -\dfrac{\lambda_3}{\lambda_1} & 0 \end{bmatrix}$ is Hurwitz. Thus, the applied control to (4.39) and (4.40) is

solution of (4.32) replacing $\mathbf{e_1}$ by $\hat{\mathbf{e}}_1$. Such an observer leads to the error

($\tilde{\mathbf{e}}_1 = \mathbf{e_1} - \hat{\mathbf{e}}_1$) dynamic of the form:

$$\begin{cases} \dot{\tilde{e}}_1(1) = \tilde{e}_1(2) - \lambda_1 \, sign(\tilde{e}_1(1)) \\ \dot{\tilde{e}}_1(2) = \tilde{e}_1(3) - \lambda_2 \, sign(\tilde{e}_1(1)) \\ \dot{\tilde{e}}_1(3) = \Delta H_1 - \lambda_3 \, sign(\tilde{e}_1(1)) \end{cases} \tag{4.42}$$

where $\Delta H_1 = H_1(\mathbf{e_1}, u_1) - H_1(\hat{\mathbf{e}}_1, u_1)$, and $sign(\tilde{e}_1(1)) = \begin{cases} 1 & if \ \tilde{e}_1(1) > 0 \\ -1 & if \ \tilde{e}_1(1) < 0 \end{cases}$.

Then, we assume that:

Assumption 2:

$\Delta H_1(\cdot)|_{\tilde{e}_1=0}$ is globally Lipschitz continuous in its first argument

$\left\| \Delta H_1(\mathbf{e_1}, u_1) \right\| \le k_3 \left\| \mathbf{e_1} \right\|$.

Assumption 3:

$\dfrac{1}{2k_3} > \left\| \mathbf{P_2^o} \right\|$, where $\mathbf{P_2^o}$ is the 2nd column of matrix $\mathbf{P^o}$ solution of (4.41).

Theorem 1: Consider the nonlinear system (4.11) with uncertain nonlinear function

$F_1(v_1, a_1)$, which is approximated as (4.24). And with control defined as in *Lamma 3*,

to which observer (4.40) is associated. Suppose *Assumption 1-3*, (4.25), and (4.31) are

satisfied. Then for any initial conditions, the state $\hat{\mathbf{e}}_1$ of the observer converges

toward the state $\mathbf{e_1}$ of the system.

Proof:

Consider the partial Lyapunov function $v = \frac{1}{2}\tilde{e}_1(1)^2$ leading to

$\dot{v} = \tilde{e}_1(1)\dot{\tilde{e}}_1(1) = \tilde{e}_1(1)[\tilde{e}_1(2) - \lambda_1 \, sign(\tilde{e}_1(1))]$, with the constraint $\left|\tilde{e}_1(2)\right|_{max} < \lambda_1$ we can

obtain $\dot{v} < \left(\left|\tilde{e}_1(2)\right| - \lambda_1\right) \cdot \left|\tilde{e}_1(1)\right| < -\sigma\left|\tilde{e}_1(1)\right|$ and $\tilde{e}(1) \to 0$ in finite time (t_1). The

remaining estimation error can then be shown to decay exponentially using Filippov's

work. Taking a convex combination of the dynamics on each side, we have

$$\begin{cases} \dot{\tilde{e}}_1(1) = \gamma(\tilde{e}_1(2) + \lambda_1) + (1-\gamma)(\tilde{e}_1(2) - \lambda_1) \\ \dot{\tilde{e}}_1(2) = \gamma(\tilde{e}_1(3) + \lambda_2) + (1-\gamma)(\tilde{e}_1(3) - \lambda_2) \\ \dot{\tilde{e}}_1(3) = \gamma(\Delta H_1 + \lambda_3) + (1-\gamma)(\Delta H_1 - \lambda_3) \end{cases} \tag{4.43}$$

For $t \geq t_1$, eliminating γ from above equations, (4.43) becomes

$$\begin{cases} \dot{\tilde{e}}_1(1) = 0 \\ \dot{\tilde{e}}_1(2) = \tilde{e}_1(3) - \frac{\lambda_2}{\lambda_1} \cdot \tilde{e}_1(2) \\ \dot{\tilde{e}}_1(3) = \Delta H_1 - \frac{\lambda_3}{\lambda_1} \cdot \tilde{e}_1(2) \end{cases} \tag{4.44}$$

Let $\mathbf{e}_1' = [\tilde{e}_1(2) \ \tilde{e}_1(3)]^T$. This is

$$\dot{\mathbf{e}}_1' = A^o \mathbf{e}_1' + [0 \ \Delta H_1(\mathbf{e}_1')]^T \tag{4.45}$$

Select Lyapunov function as $V^o = \mathbf{e}_1'^T \mathbf{P}^o \mathbf{e}_1'$,

$\dot{V}^o = 2\mathbf{e}_1'^T \mathbf{P}^o \dot{\mathbf{e}}_1' = 2\mathbf{e}_1'^T \mathbf{P}^o (\mathbf{A}^o \mathbf{e}_1' + [0 \ \Delta H_1(\cdot)]^T) = 2\mathbf{e}_1'^T \mathbf{P}^o \mathbf{A}^o \mathbf{e}_1' + 2\mathbf{e}_1'^T \mathbf{P}^o [0 \ \Delta H_1(\cdot)]^T$

$= -\mathbf{e}_1'^T \mathbf{I} \mathbf{e}_1' + 2\mathbf{e}_1'^T \mathbf{P}_2^o \Delta H_1(\cdot) = -\left\|\mathbf{e}_1'\right\|^2 + 2\mathbf{e}_1'^T \mathbf{P}_2^o \Delta H_1(\cdot) \tag{4.46}$

$\dot{V}^o \leq -\left\|\mathbf{e}_1'\right\|^2 + 2\left\|\mathbf{e}_1'\right\|\left\|\mathbf{P}_2^o\right\|\left\|\Delta H(\cdot)\right\| \leq -\left\|\mathbf{e}_1'\right\|^2 + 2\left\|\mathbf{e}_1'\right\|\left\|\mathbf{P}_2^o\right\|k_3\left\|\mathbf{e}_1'\right\|$

$\dot{V}^o \leq -(1 - 2k_3\left\|\mathbf{P}_2^o\right\|)\left\|\mathbf{e}_1'\right\|^2 \leq 0$

and thus ensures that $\mathbf{e}_1'$ decreases to zero

Remark:

In many applications, the $sign(\tilde{e}_1(1))$ in (4.42) is replaced by a saturation function of

the form

$$sat(\tilde{e}_1(1)) = \begin{cases} sign(\tilde{e}_1(1)) & if \; |\tilde{e}_1(1)| > \varphi^O \\ \tilde{e}_1(1)/\phi^O & if \; |\tilde{e}_1(1)| < \varphi^O \end{cases}$$

in order to remedy the control chattering [24].

Naturally, to prove asymptotic stabilization of the controlled plant plus the

observer, we use the following Lyapunov function :

$$W = \frac{1}{2}\hat{s}^2 + \frac{1}{2}\mathbf{e}_1''^{T}\mathbf{P}\mathbf{e}_1'' + \frac{1}{2}\tilde{\boldsymbol{\theta}}^{T}\boldsymbol{\Gamma}^{-1}\tilde{\boldsymbol{\theta}} \tag{4.47}$$

where $\tilde{\boldsymbol{\theta}} = \boldsymbol{\theta}^* - \hat{\boldsymbol{\theta}}$, and $\mathbf{e}_1'' = [\hat{e}_1(1) \quad \hat{e}_1(2)]^T$. Let $\hat{s} = \lambda^2 \hat{e}_1(1) + 2\lambda \hat{e}_1(2) + \hat{e}_1(3)$.

The time derivative of (4.47) is

$$\dot{W} = \hat{s}\dot{\hat{s}} + \frac{1}{2}\mathbf{e}_1''^{T}\mathbf{P}\dot{\mathbf{e}}_1'' + \frac{1}{2}\dot{\mathbf{e}}_1''^{T}\mathbf{P}\mathbf{e}_1'' + \frac{1}{2}\tilde{\boldsymbol{\theta}}^{T}\boldsymbol{\Gamma}^{-1}\dot{\tilde{\boldsymbol{\theta}}} + \frac{1}{2}\dot{\tilde{\boldsymbol{\theta}}}^{T}\boldsymbol{\Gamma}^{-1}\tilde{\boldsymbol{\theta}}$$

$$= \hat{s}[\lambda^2 \dot{\hat{e}}_1(1) + 2\lambda \dot{\hat{e}}_1(2) + \dot{\hat{e}}_1(3)] + \mathbf{e}_1''^{T}\mathbf{P}(\mathbf{A}_1\mathbf{e}_1'' + [0 \;\; \hat{s}]^T) + \tilde{\boldsymbol{\theta}}^{T}\boldsymbol{\Gamma}^{-1}(-\dot{\hat{\boldsymbol{\theta}}})$$

$$= \hat{s}[\lambda^2 \hat{e}_1(2) + 2\lambda \hat{e}_1(3) + \boldsymbol{\theta}^{*T}\varphi(\hat{\mathbf{e}}_1) + G_1\hat{u}_1 + w] + \frac{1}{2}\mathbf{e}_1''^{T}(\mathbf{P}\mathbf{A}_1 + \mathbf{A}_1^{T}\mathbf{P})\mathbf{e}_1'' + \mathbf{e}_1''^{T}\mathbf{P}[0 \;\; \hat{s}]^T + \tilde{\boldsymbol{\theta}}^{T}\boldsymbol{\Gamma}^{-1}(-\dot{\hat{\boldsymbol{\theta}}})$$

$$= \hat{s}[\lambda^2 \hat{e}_1(2) + 2\lambda \hat{e}_1(3) + \boldsymbol{\theta}^{*T}\varphi(\hat{\mathbf{e}}_1) + G_1\hat{u}_1 + w] - \frac{1}{2}\mathbf{e}_1''^{T}\mathbf{Q}\mathbf{e}_1'' + \hat{s}(\hat{e}_1(1)p_{12} + \hat{e}_1(2)p_{22}) - \tilde{\boldsymbol{\theta}}^{T}\boldsymbol{\Gamma}^{-1}\dot{\hat{\boldsymbol{\theta}}}$$

$$\tag{4.48}$$

Apply $\hat{u}_1 = G_1^{-1}[-\hat{\boldsymbol{\theta}}^T\varphi(\hat{\mathbf{e}}_1) - \lambda^2 \hat{e}_1(2) - 2\lambda \hat{e}_1(3) - p_{21}\hat{e}_1(1) - p_{22}\hat{e}_1(2) - k \; sign(\hat{s}(\hat{\mathbf{e}}_1;t))]$

to (4.48), and let $k = k_2 + w^u$, we have following relationship:

42

$$\dot{W} = \hat{s}[\tilde{\boldsymbol{\theta}}^T \varphi(\hat{\mathbf{e}}_1) - p_{21}\hat{e}_1(1) - p_{22}\hat{e}_1(2) - k \; sign(\hat{s}(\hat{\mathbf{e}}_1;t)) + w] - \frac{1}{2}\mathbf{e}_1''^{\mathbf{T}}\mathbf{Q}\mathbf{e}_1'' + \hat{s}(\hat{e}_1(1)p_{21} + \hat{e}_1(2)p_{22}) - \tilde{\boldsymbol{\theta}}^T \boldsymbol{\Gamma}^{-1}\dot{\hat{\boldsymbol{\theta}}}$$

$$= \hat{s}[\tilde{\boldsymbol{\theta}}^T \varphi(\hat{\mathbf{e}}_1) - k \; sign(\hat{s}(\hat{\mathbf{e}}_1;t)) + w] - \frac{1}{2}\mathbf{e}_1''^{\mathbf{T}}\mathbf{Q}\mathbf{e}_1'' - \tilde{\boldsymbol{\theta}}^T\boldsymbol{\Gamma}^{-1}(\boldsymbol{\Gamma}\hat{s}\varphi(\hat{\mathbf{e}}_1))$$

$$= \hat{s}[-(k_2 + w'')sign \; (\hat{s}) + w] - \frac{1}{2}\mathbf{e}_1''^{\mathbf{T}}\mathbf{Q}\,\mathbf{e}_1''$$

$$< \; -k_2|\hat{s}| - \frac{1}{2}\mathbf{e}_1''^{\mathbf{T}}\mathbf{Q}\mathbf{e}_1'' \; < \; -k_2|\hat{s}| \; < \; 0 \qquad\qquad (4.49)$$

This completes the proof.

4.6 Simulation Results

To examine the behavior of a platoon of vehicles under the above controller, we run simulations for a platoon consisting of 3 different types of vehicles again. Three types of vehicles with their relevant parameters are the same to the ones shown in the Table. 3-2 and are used in the simulations. In the simulation conducted, all the vehicles are assumed to be initially traveling at the steady-state velocity of $v_0 = 17.9$ m/s (i.e., 40 mph). Beginning at time $t = 0$ s, the lead vehicle's velocity is increased from its steady-state velocity value of 17.9 m/s until it reaches its final value of 21.9 m/s (i.e., 50 mph): the maximum jerk and the peak acceleration values corresponding to this velocity time profile are 0.5 m/s^3 and 1m/s^2 , respectively (also see Fig. 3-4 and Fig. 3-5). Take three following vehicles as an simulation example, the order of vehicles in the platoon followed the lead vehicle is as follows: Daihatsu Charade CLS followed by Buick Regal Custom followed by BMW 750iL. Consider the vehicle

loading, total mass of each following vehicle is conditioned by adding vehicle curb

mass and passengers' mass. From Fig. 4-5 to Fig. 4-9 are the simulations of the

application using a sliding mode controller with the boundary layer. From Fig. 4-10 to

Fig. 4-14, we can see that the fuzzy neural approximator can approximate the

uncertain nonlinear term of the system. From Fig. 4-15 to Fig. 4-19 , we apply the

H_∞ performance with the control law obtained in section 4.3. It shows that the

performance is better and the chattering is attenuated, too. From Fig. 4-20 to Fig. 4-24,

the observer is associated to estimate the system states, it shows that performance is

still acceptable.
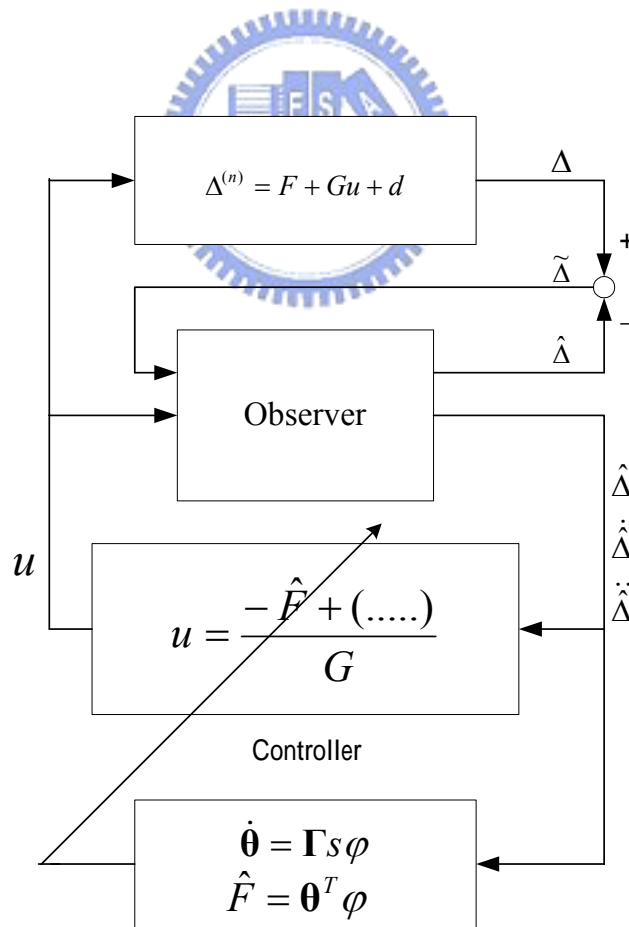
Fig. 4-4 Block Diagram of Overall System

symbols	parameters(values)
λ	1
λ_1	1
λ_2	2
λ_3	1
k	1.2
ρ	0.3
P_{21}	0.5
P_{22}	1.5
ϕ	1.0
$\hat{\Delta}_1 \mid_{t=0}$	-0.1
$\hat{\Delta}_2 \mid_{t=0}$	0.2
$\hat{\Delta}_3 \mid_{t=0}$	0.1
Γ_1	50$\mathbf{I}$
Γ_2	40$\mathbf{I}$
Γ_3	40$\mathbf{I}$

Table. 4-1 Simulation Model Parameters of Modified Sliding Mode Control
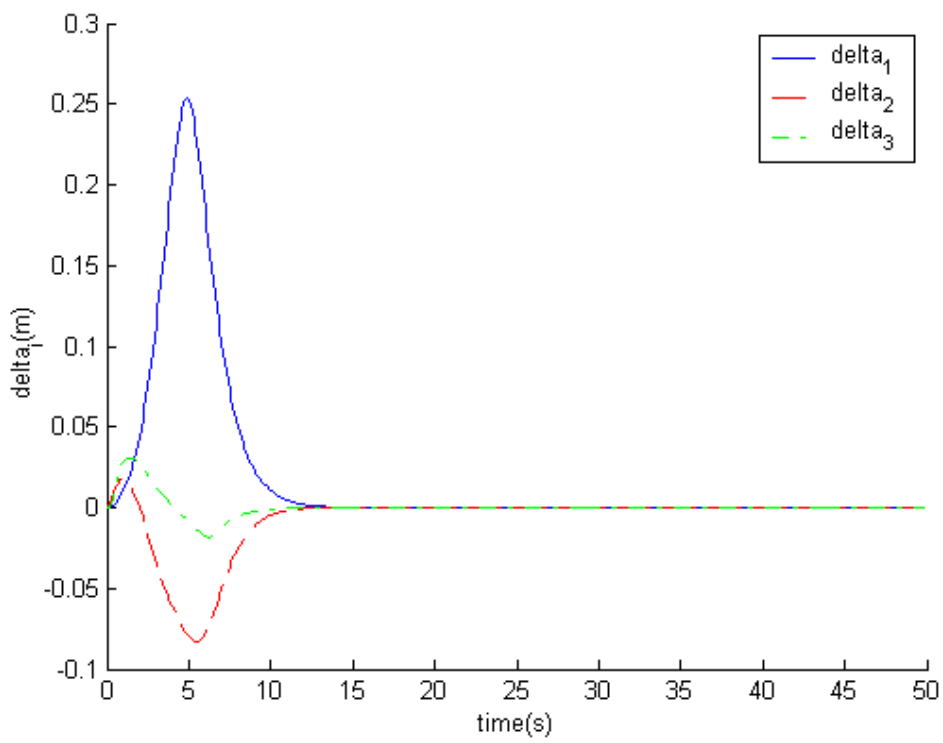
Fig. 4-5 $\Delta_1, \Delta_2, and \Delta_3$ **versus** *t*
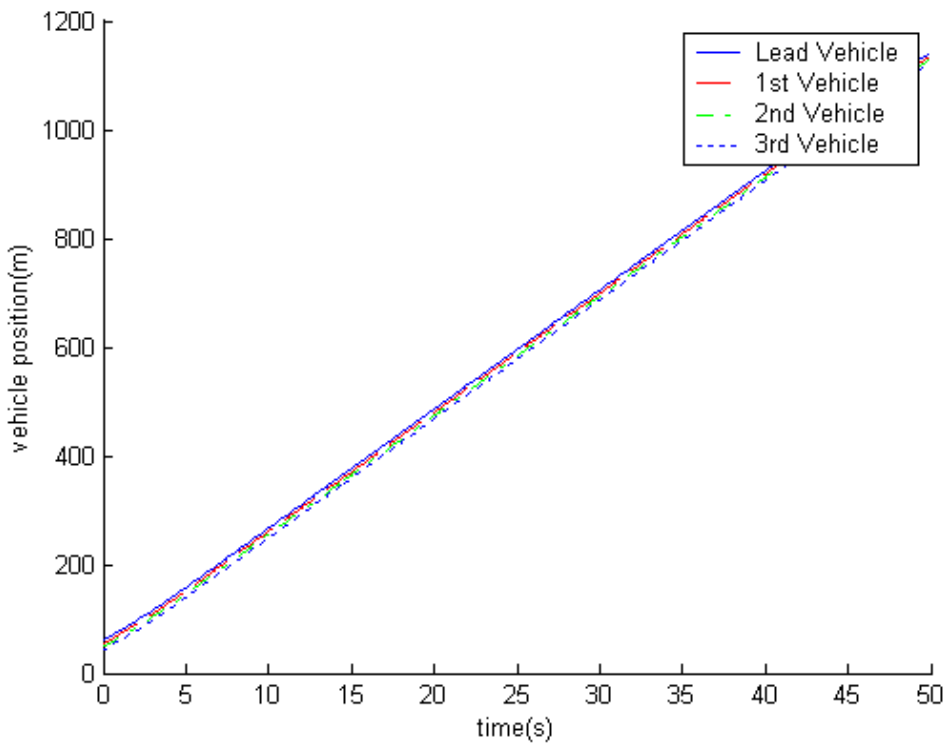
Fig. 4-6 $p_l, p_1, p_2, and p_3$ **versus** *t*
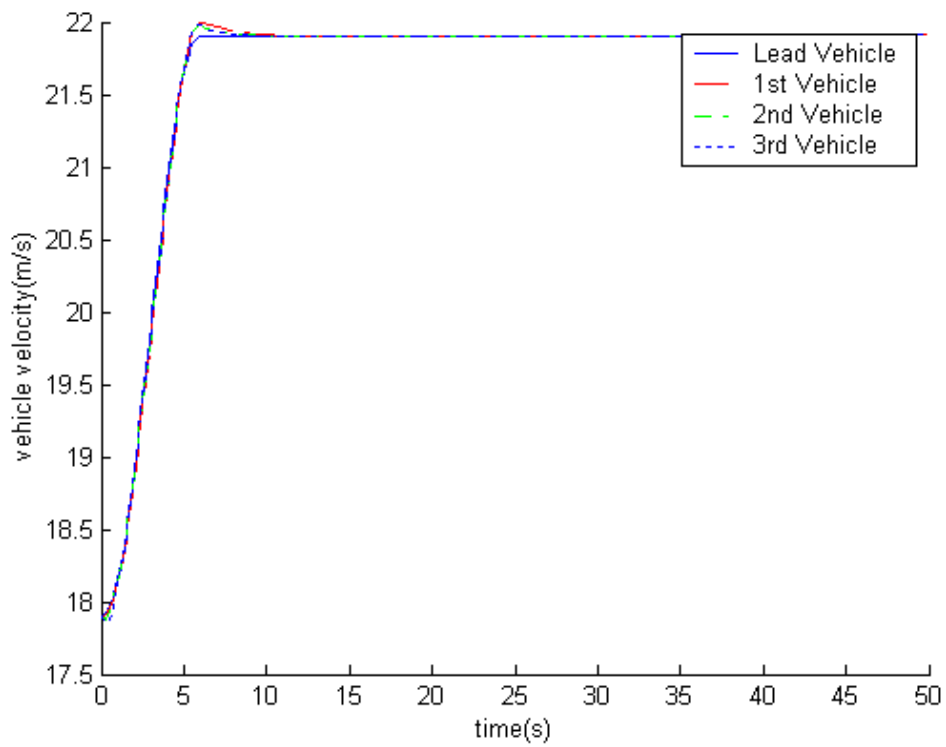
Fig. 4-7 $v_l, v_1, v_2, and\ v_3$ **versus** t
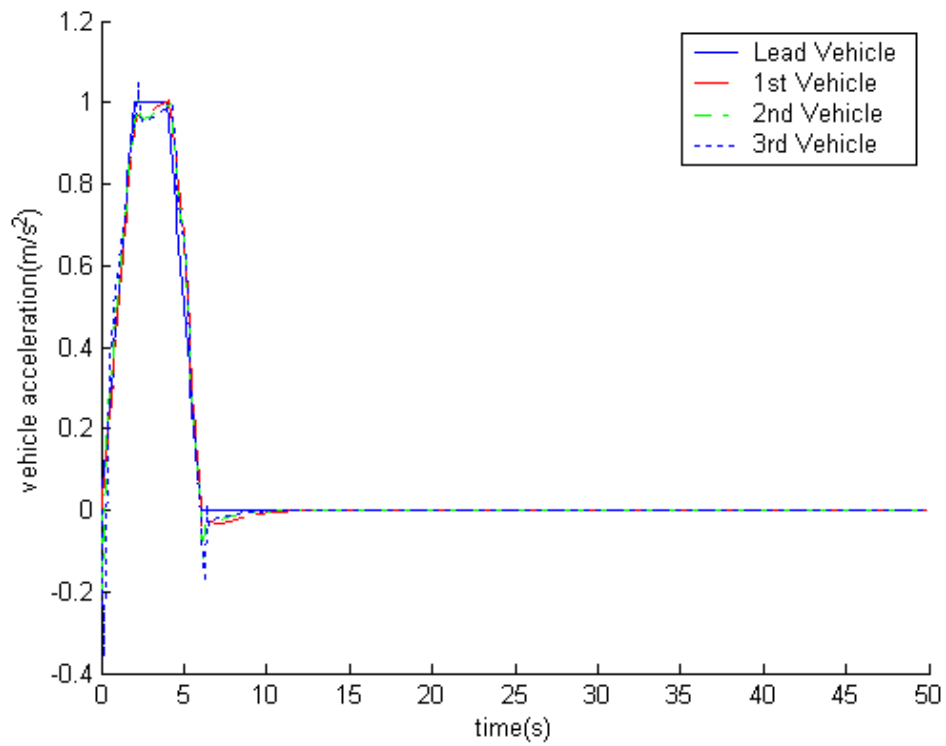
Fig. 4-8 $a_l, a_1, a_2, and\ a_3$ **versus** t

47
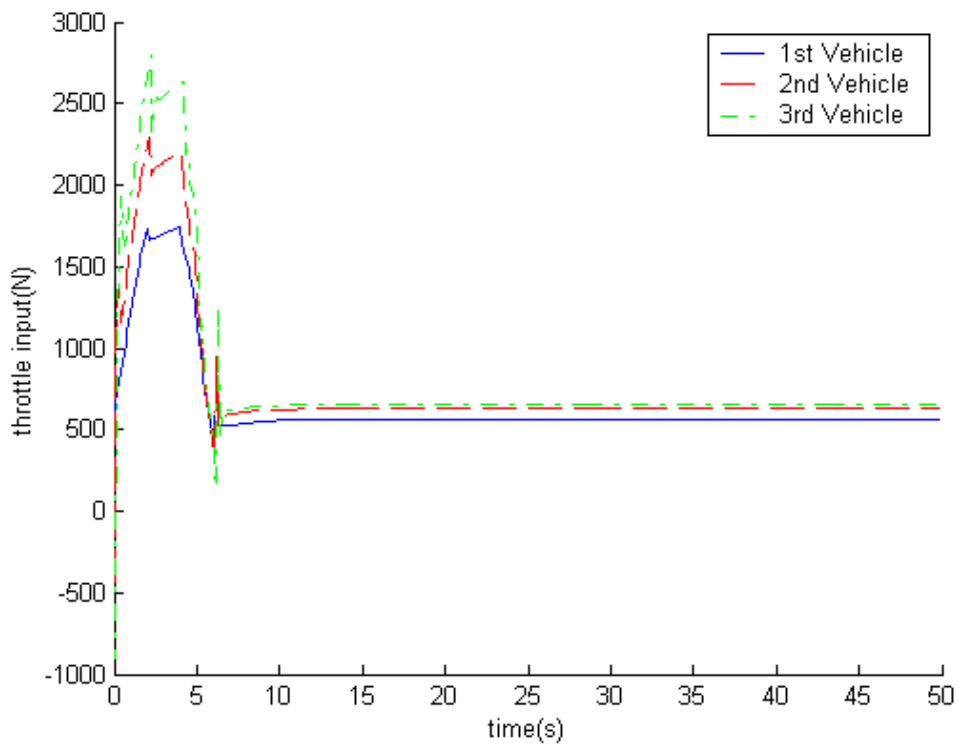
Fig. 4-9 $u_1, u_2, and\ u_3$ **versus** t
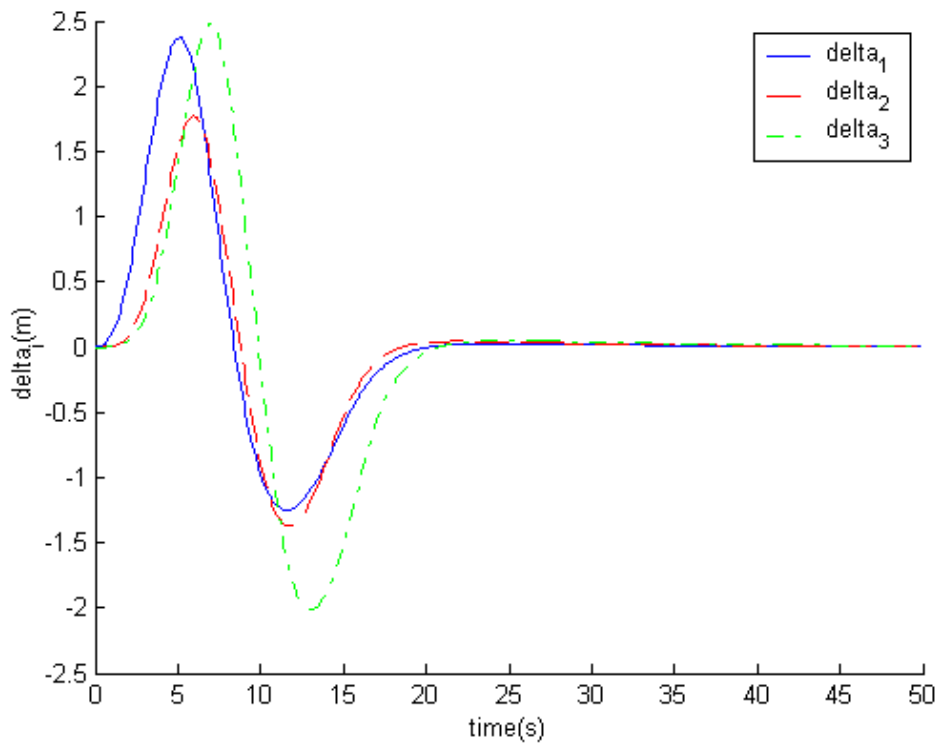
Fig. 4-10 $\Delta_1, \Delta_2, and\ \Delta_3$ **versus** t
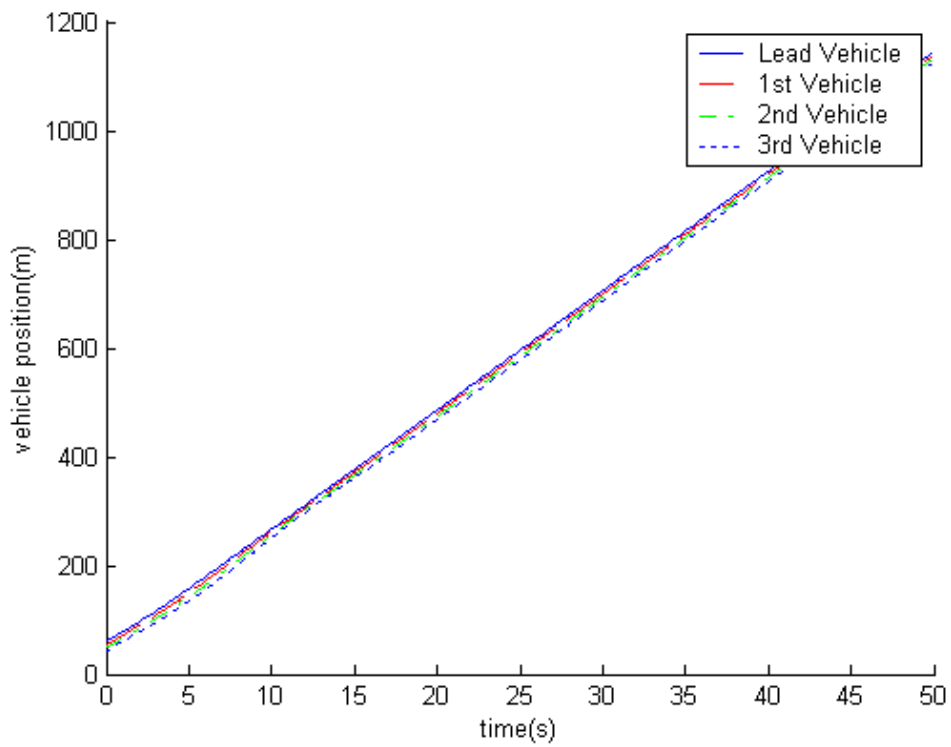
Fig. 4-11 p_l, p_1, p_2, and p_3 **versus** t
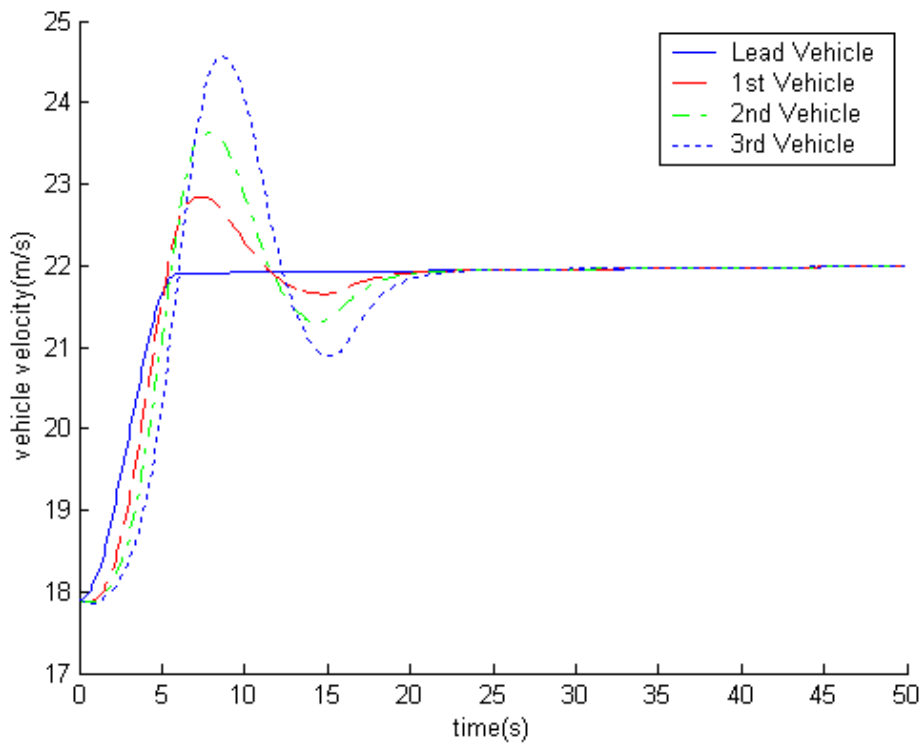
Fig. 4-12 v_l, v_1, v_2, and v_3 **versus** t

49
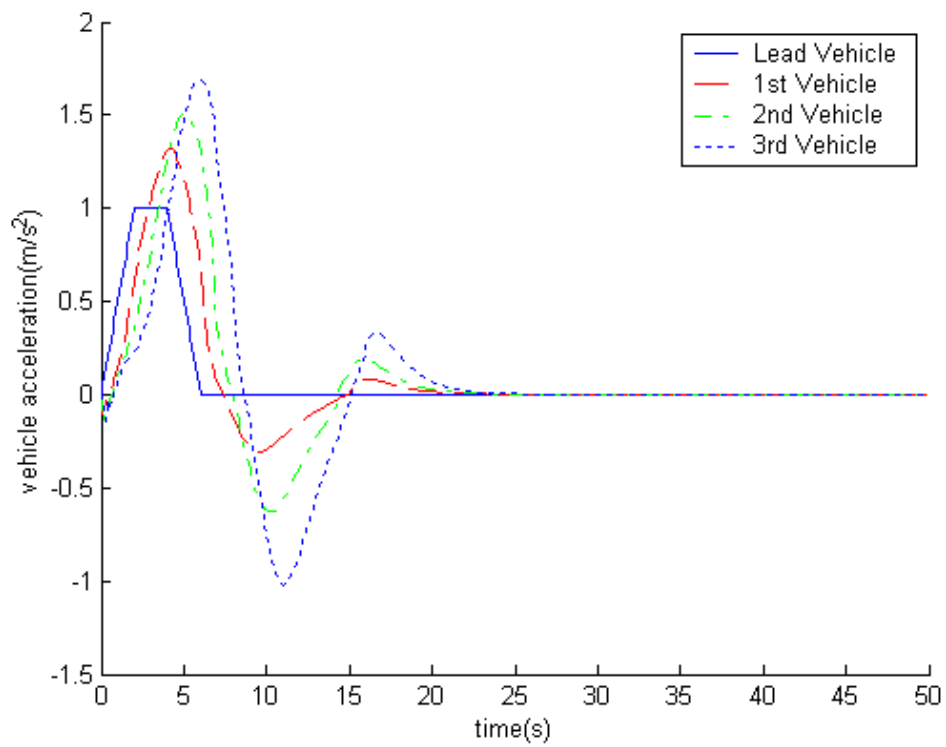
Fig. 4-13 a_l, a_1, a_2, and a_3 versus t
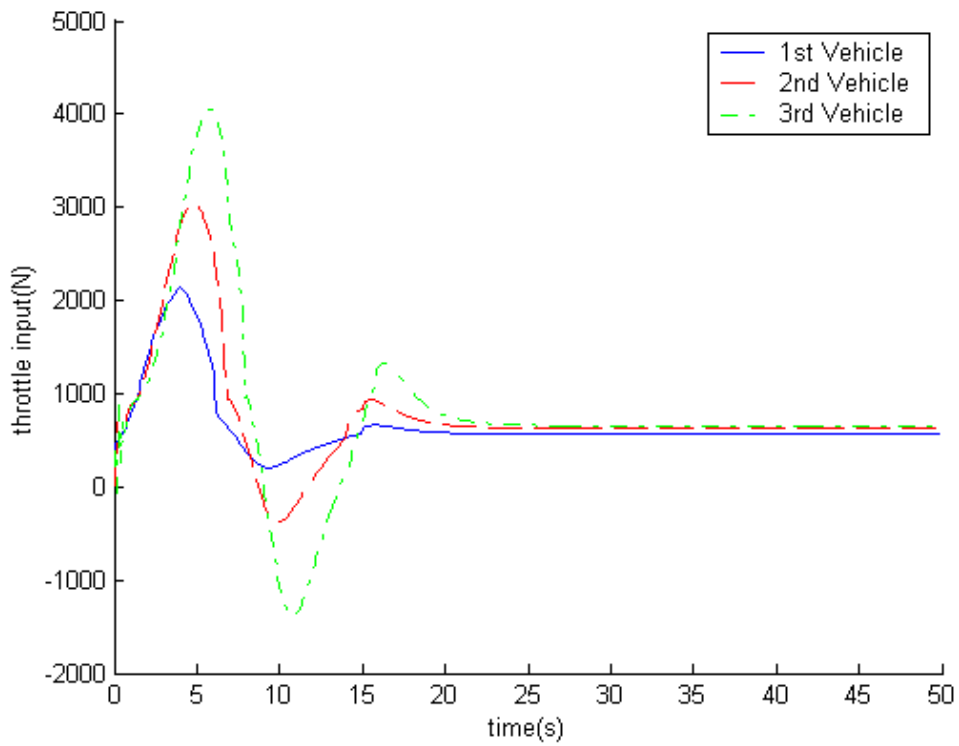
Fig. 4-14 u_1, u_2, and u_3 versus t
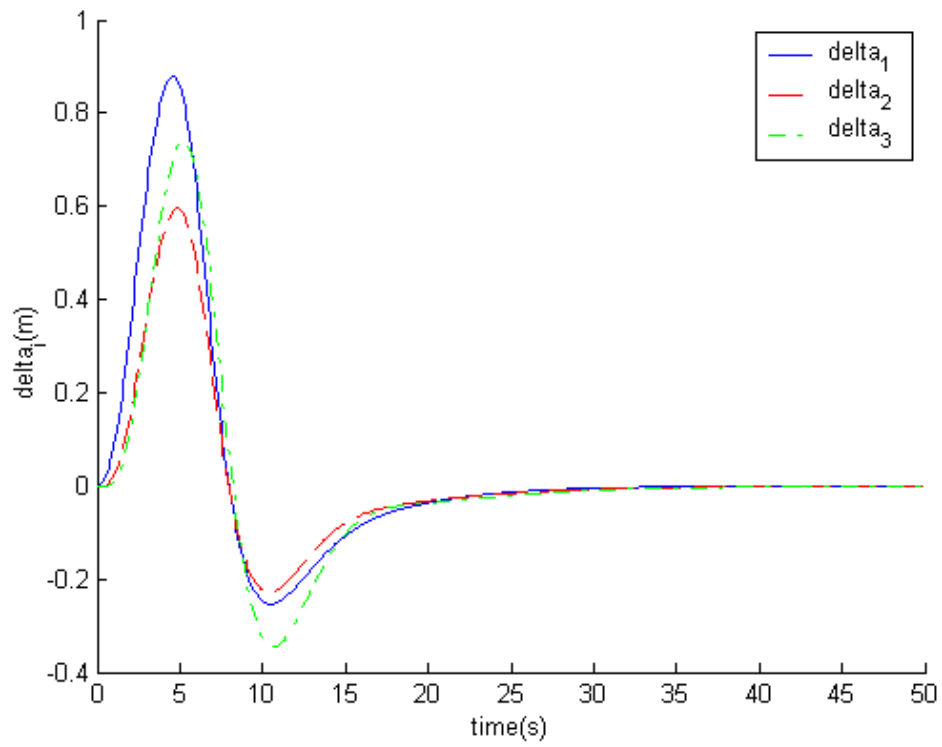
Fig. 4-15 $\Delta_1, \Delta_2, and\ \Delta_3$ **versus** *t*
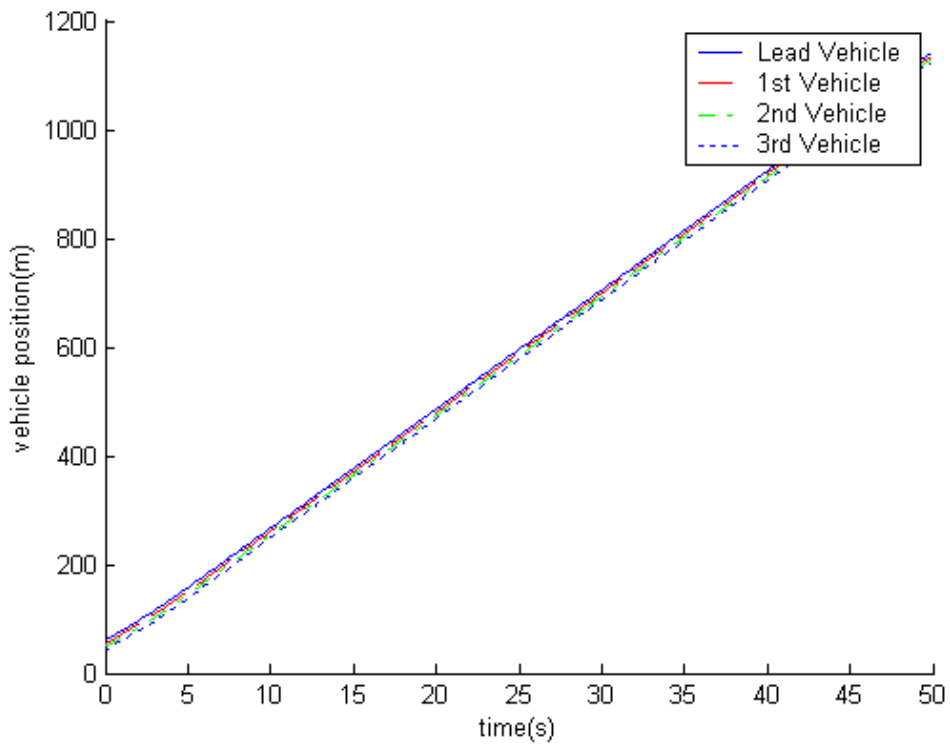
Fig. 4-16 $p_l, p_1, p_2, and\ p_3$ **versus** *t*
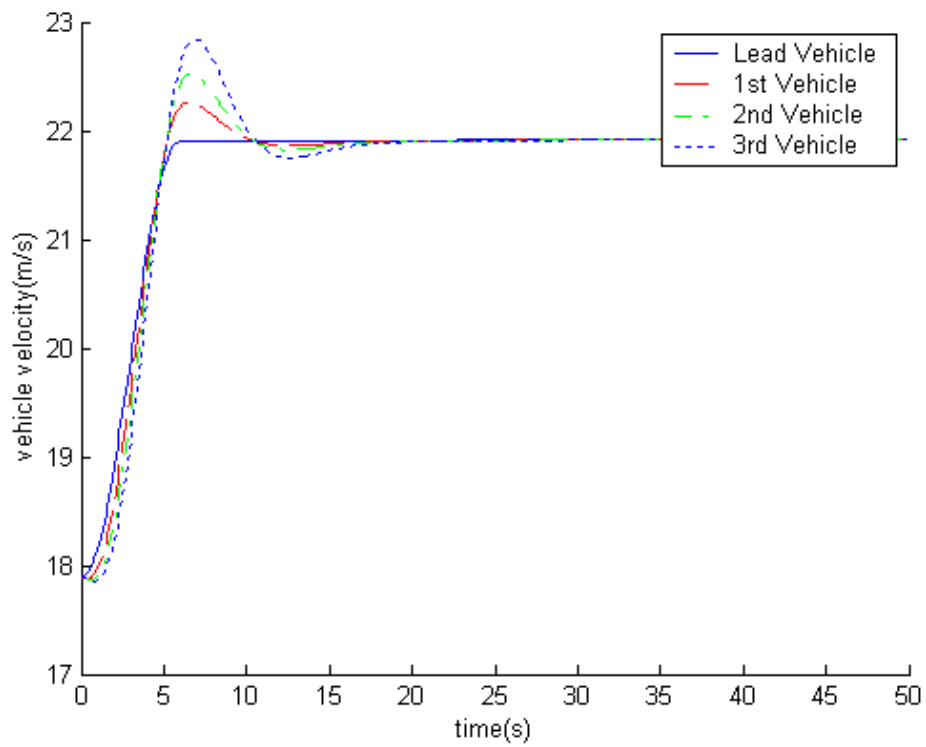
Fig. 4-17 $v_l, v_1, v_2, and\ v_3$ **versus** t
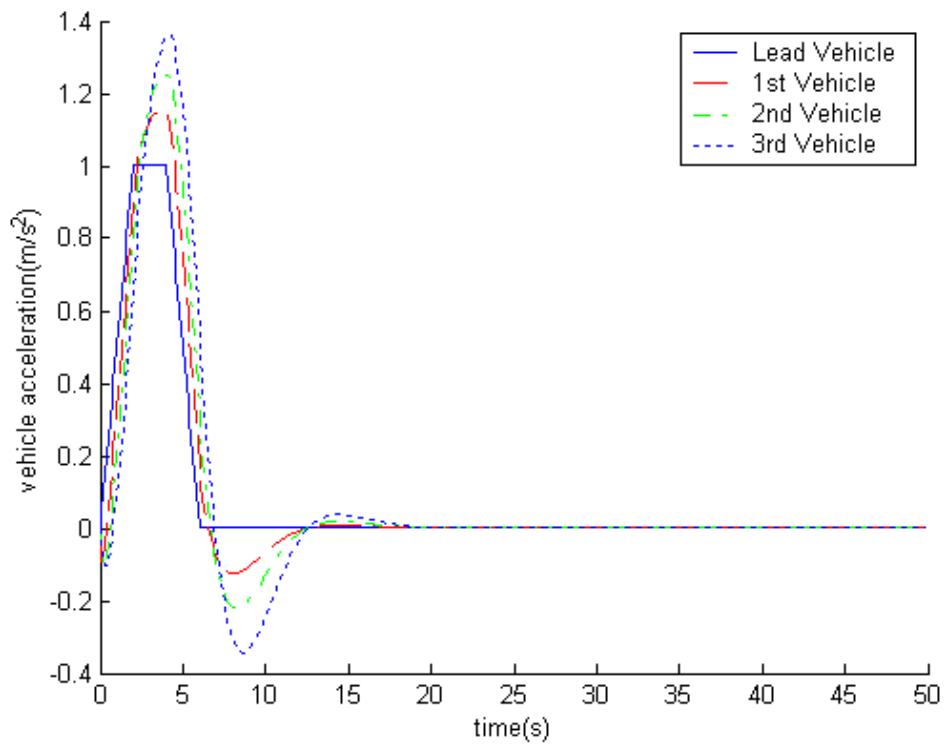
Fig. 4-18 $a_l, a_1, a_2, and\ a_3$ **versus** t
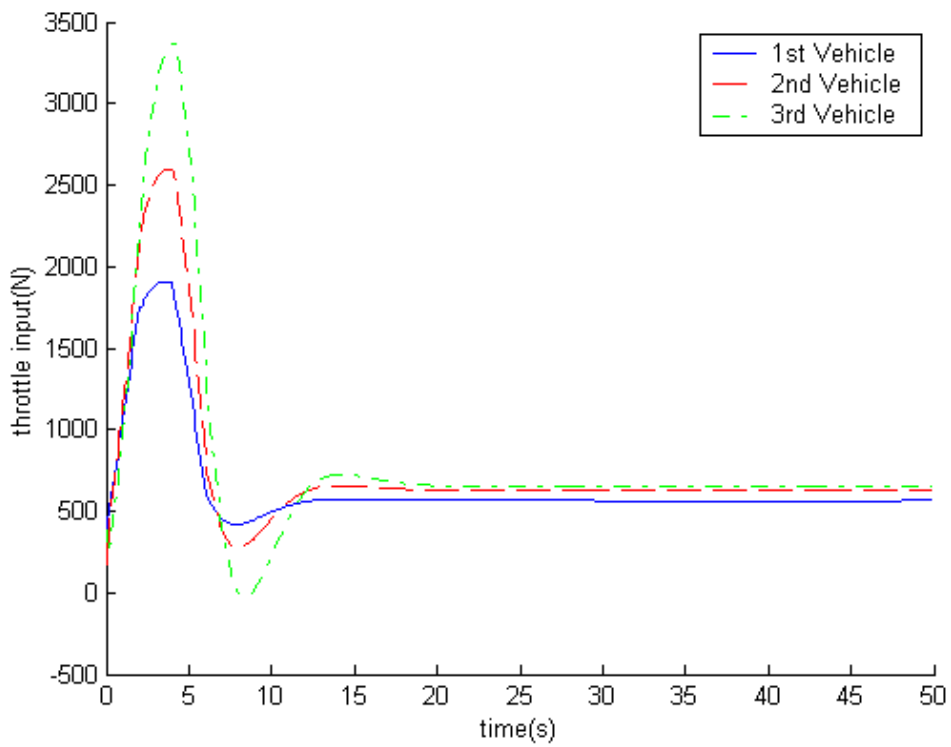
Fig. 4-19 $u_1, u_2, and\ u_3$ **versus** t
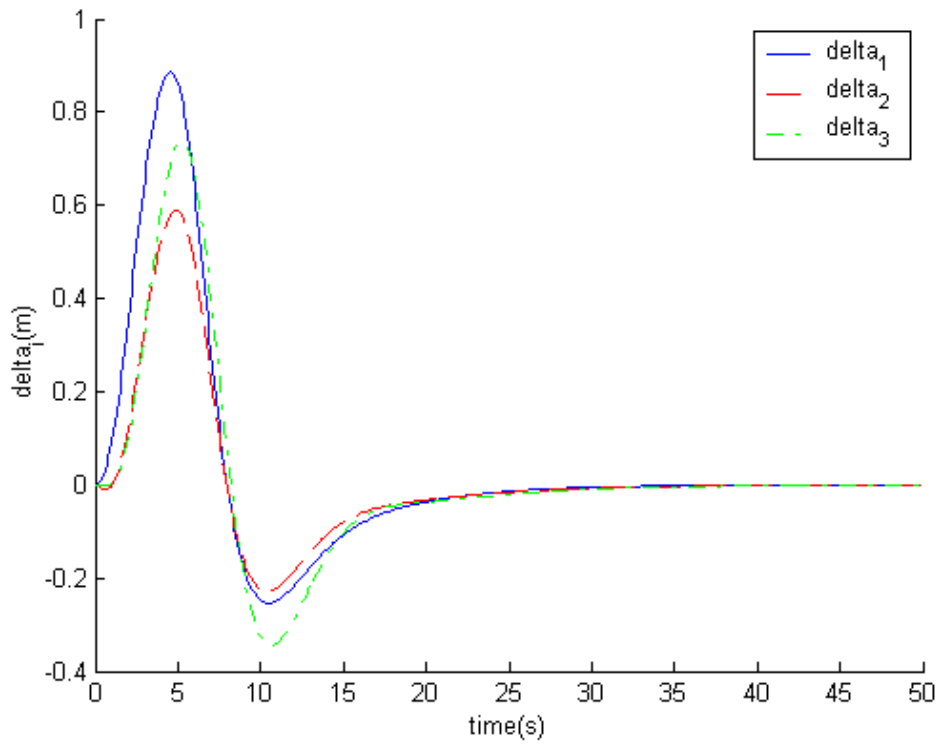
Fig. 4-20 $\Delta_1, \Delta_2, and\ \Delta_3$ **versus** t
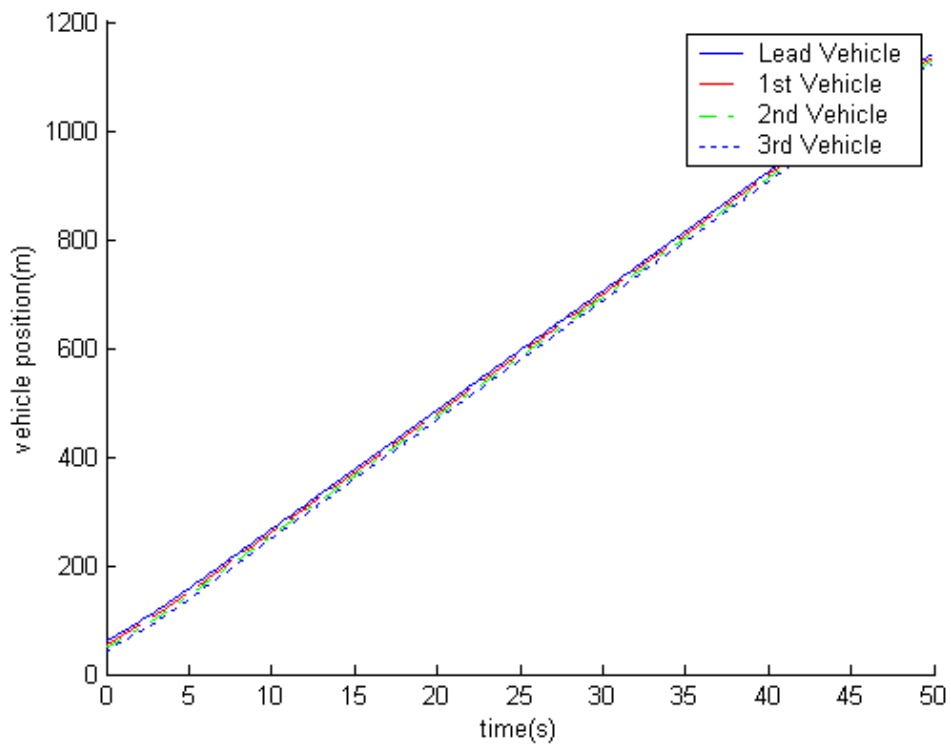
Fig. 4-21 $p_l, p_1, p_2, and\ p_3$ **versus** t
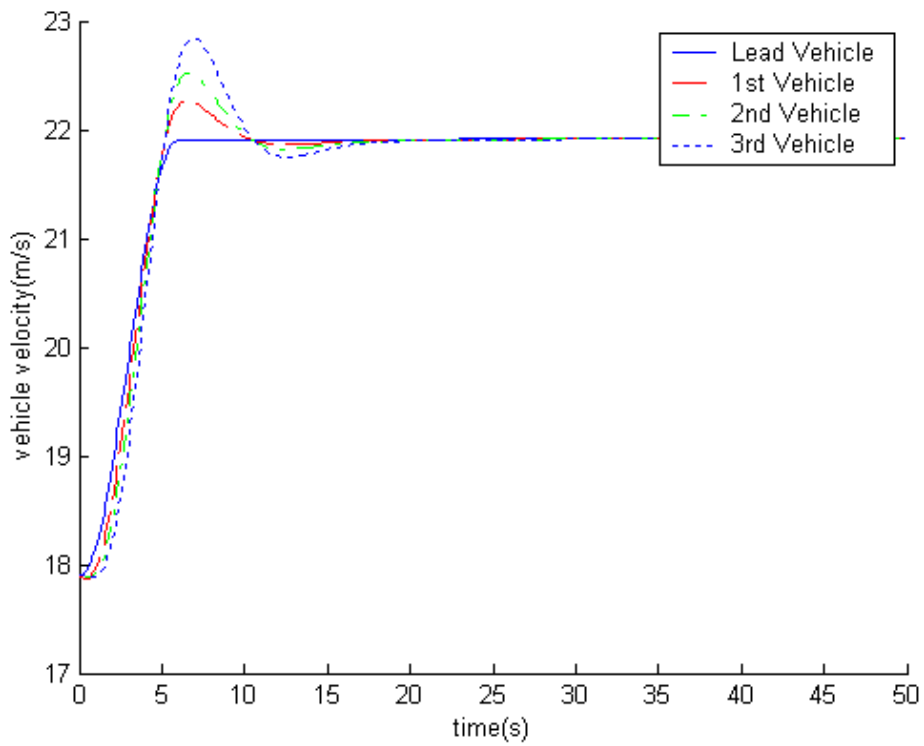
Fig. 4-22 $v_l, v_1, v_2, and\ v_3$ **versus** t

54
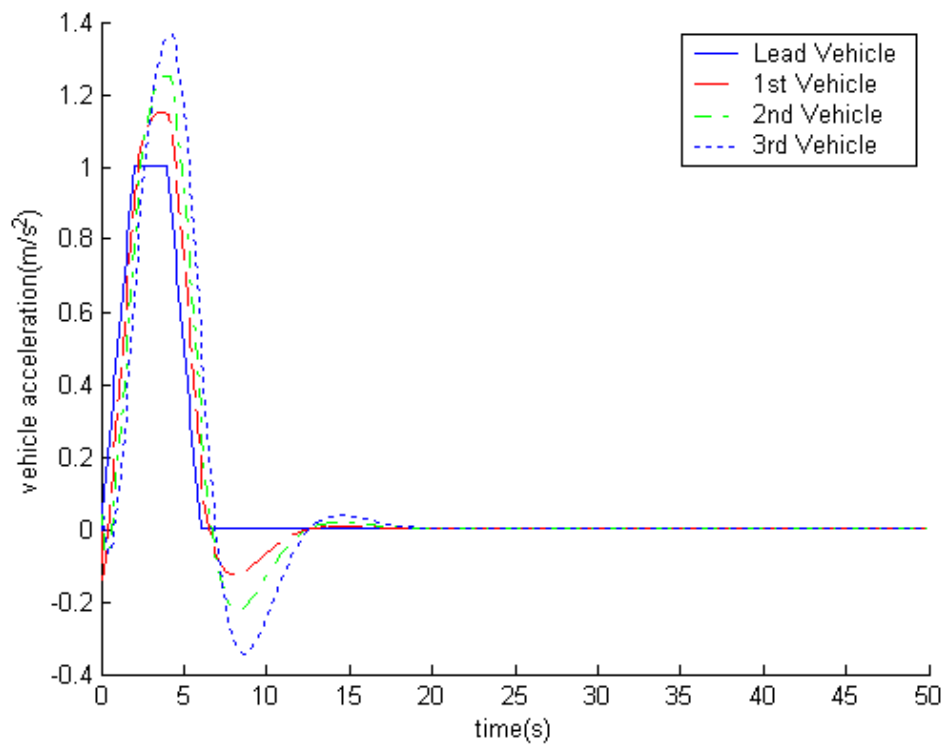
Fig. 4-23 $a_l, a_1, a_2, and\ a_3$ **versus** t
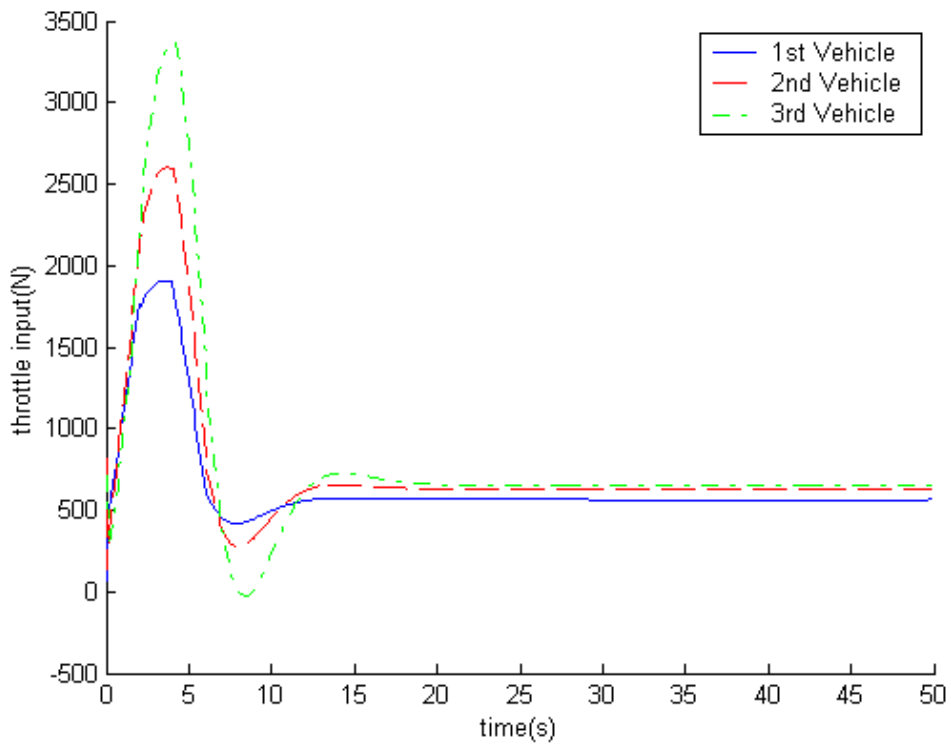

Fig. 4-24 $u_1, u_2, and\ u_3$ **versus** t

55

Chapter 5   Conclusions

In this thesis, we modeled mathematically both vehicle and car-following systems. In order to gain better performance and ensure the robustness and global stability, a sliding mode controller with the fuzzy-neural network approximator and H_∞ performance was proposed. Moreover, considering the technical difficulties and the economic benefits, we assumed that only the relative distance of two vehicles was measurable. Thus, an observer-based modified sliding mode controller was developed.

The control performance of the proposed system were simulated. Simulation results demonstrated the validity and effectiveness of the controlled systems. The system with the modified sliding mode controller showed a better performance than the one controlled by a sliding mode controller did. With these two controllers, the robustness and the global stability were both guaranteed during the vehicles-following process in the presence of the uncertainties and disturbances.

In designing the output feedback control law of an observer-based modified sliding mode controller, no differentiation of system outputs was performed in order to avoid the noise amplification associated with numerical differentiation, and no knowledge on nonlinearities of the nonlinear parts of the system was required. This

controller is subject to on-line tuning for a nonlinear system. Although the performance

of the car-following system with an observer is not as good as the one with a modified

sliding mode controller which were combined with an aprroximator and H_∞

performance conception, it is still satisfying.

References

[1] Shahab Sheikholeslam and Charles A. Desoer, "Longitudinal control of a platoon of vehicles with no communication of lead vehicle information: a system level study," *IEEE Transactions on Vehicular Technology*, Vol. 42, No. 4, pp.546-554, November 1993.

[2] Michel Fliess, "Generalized controller canonical forms for linear and nonlinear dynamics," *IEEE Transactions on Automatic Control*, Vol. 35, No. 9, pp.994-1001, September 1990.

[3] W. Perruquetti, T. Floquet, and P. Borne, "A note on sliding observer and controller for generalized canonical forms," *Decision and Control, Proceedings of the 37th IEEE Conference on* , Vol. 2 , pp.1920-1925, December 1998.

[4] Thomas D. Gillespie, *Fundamentals of Vehicle Dynamics*, Warrendale, PA./Society of Automatic Engineers,Inc. 1992.

[5] Wei-Yen Wang, Mei-Lang Chan, Chen-Chien James Hsu, and Tsu-Tian Lee, "H_∞ tracking-based sliding mode control for uncertain nonlinear systems via an adaptive fuzzy-neural approach," *IEEE Transactions on Systems, Man, and Cybernetics – Part B: Cybernetics*, Vol. 32, No. 4, pp.483 – 492, August 2002.

[6]   , *Fuzzy   :   ,
         , 83   10

[7] Shahab Sheikholeslam and Charles A. Desoer, "A system level study of the logitudinal control of a platoon of vehicles," *ASME J. Dynamic Systems, Measurement, and Control*, Vol. 114, pp.286-292, June 1992.

[8] Shahab Sheikholeslam and Charles A. Desoer, "Combined longitudinal and lateral control of a platoon of vehicles: a system level study," *PATH Technical Memorandum 91-3*, September 1991.

[9] Bor-Sen Chen, Ching-Hsiang Lee, and Yeong-Chan Chang, " H_∞ tracking design of uncertain nonlinear SISO systems: Adaptive fuzzy approach," *IEEE Transactions on Fuzzy Systems*, Vol. 6, No. 1, pp.32-43, February 1996.

[10] Wei-Yen Wang, Mei-Lang Chan, Tsu-Tian Lee, and Cheng-Hsin Liu, "Adaptive fuzzy control for strict-feedback canonical nonlinear systems with H_∞ tracking performance," *IEEE Transactions on Systems, Man, and Cybernetics – Part B: Cybernetics*, Vol. 30, No. 6, pp.878 – 885, December 2000.

[11] J. J. E. Slotine and Weiping Li, *Applied nonlinear control*, Englewood Cliffs, NJ: Prentice-Hall, 1991.

[12] D. Yanakiev and I. Kanellakopoulos, "Longitudinal control of heavy-duty vehicles for automated highway systems," *Proceedings of the American Control Conference ,* Vol. 5, pp:3096-3100, June 1995

[13] L. X. Wang, *Adaptive fuzzy systems and control: design and stability analysis,*

Englewood Cliffs, NJ: Prentice-Hall, 1994.

[14] M. Tai and M. Tomizuka, "Robust longitudinal velocity tracking of vehicles using traction and brake control," *Advanced Motion Control*, *Proceedings of the 6th International Workshop on*, pp:305 – 310, March/April 2000.

[15] D. N. Godbole and J. Lygeros, "Longitudinal control of the lead car of a platoon," *IEEE Transactions on Vehicular Technology*, Vol. 43, No. 4, pp.1125-1135, November 1994.

[16] Chin-Teng Lin and C. S. George Lee, *Neural fuzzy systems: a neuro-fuzzy synergism to intelligent systems*, Upper Saddle River, NJ: Prentice Hall PTR, 1995

[17]   ,   ,   , 88   9

[18] W. Wang, "Modeling scheme for vehicle longitudinal control," *Proceedings of the 31st IEEE Conference on Decision and Control*, Vol. 1, pp:549-554, December 1992.

[19] J. T. Spooner and K. M. Passino, "Stable adaptive control using fuzzy systems and neural networks," *IEEE Transactions on Fuzzy Systems*, Vol. 4, pp.339-359, June 1996.

[20] Li-Xin Wang, "Stable adaptive fuzzy controllers with application to inverted pendulum tracking," *IEEE Transactions on Systems, Man, and Cybernetics –*

Part B: Cybernetics, Vol. 26, No. 5, pp.677-691, October 1996.

[21] Li-Xin Wang, "Stable adaptive fuzzy control of nonlinear systems," *IEEE Transactions on Fuzzy Systems*, Vol. 1, No. 2, pp.146-155, May 1993.

[22] Chih-Min Lin, C. F. Hsu, "Self-learning fuzzy sliding-mode control for antilock bracking systems," *IEEE Transactions on Control Systems Technology*, Vol. 11, No. 2, pp.273-278, March 2003.

[23] T. Hessberg, M. Tomizuka, "Fuzzy logic control for lateral vehicle guidance," *Second IEEE Conference on Control Applications*, Vol. 2, pp.581-586, September 1993.

[24] Y. G. Leu, T. T. Lee, and W. Y. Wang, "Observer-based adaptive fuzzy-neural control for unknown nonlinear dynamical systems," *IEEE Transactions on Systems, Man, and Cybernetics – Part B: Cybernetics*, Vol. 29, No. 5, pp.583-591, October 1999.

[25] C. C. Lee, "Fuzzy logic in control system: fuzzy logic controller-part I," *IEEE Transactions on Systems, Man, and Cybernetics*, Vol. 20, pp.404-418, March/April 1990.

[26] C. C. Lee, "Fuzzy logic in control system: fuzzy logic controller-part II," *IEEE Transactions on Systems, Man, and Cybernetics*, Vol. 20, pp.419-435, March/April 1990.

[27] K. S. Tsakalis and P. A. Ioannou, *Linear Time-Varying Systems*. Englewood Cliffs, NJ: Prentice-Hall, 1993.

[28] Byung-Jae Choi, Seong-Woo Kwak, and Byung Kook Kim, "Design and stability analysis of single-input fuzzy logic controller," *IEEE Transactions on Systems, Man, and Cybernetics*, Vol. 30, No. 2, pp.303-309, April 2000.

[29] Ji-Chang Lo and Ya-Hui Kuo, "Decoupled fuzzy sliding-mode control," *IEEE Transactions on Fuzzy Systems*, Vol. 6, No. 3, pp.426-435, August 1998.

[30] Jacob S. Glower and Jeffrey Munighan, "Designing fuzzy controllers from a variable structures standpoint," *IEEE Transactions on Fuzzy Systems*, Vol. 5, No. 1, pp.138-144, February 1997.

[31] Byungkook Yoo and Woonchul Ham, "Adaptive fuzzy sliding mode control of nonlinear system," *IEEE Transactions on Fuzzy Systems*, Vol. 6, No. 2, pp.315-321, May 1998.

[32] Iqbal Husain, Sameer Sodhi, and Mehrdad Ehsani, "A sliding mode observer based controller for switched reluctance motor drives," *Industry Applications Society Annual Meeting , Conference Record of the 1994 IEEE ,* Vol. 1, pp.635-643, October 1994.

[33] Cem Unsal and Pushkin Kachroo, "Sliding mode measurement feedback control for antilock braking systems," *IEEE Transactions on Control Systems*

Technology, Vol. 7, No. 2, pp.271-281, March 1999.

[34] N. J. Schouten, M. A. Salman, and N. A. Kheir, "Fuzzy logic control for parallel hybrid vehicles," *IEEE Transactions on Control Systems Technology*, Vol. 10, No. 3, pp.460-468, May 2002.

[35] N. Jalil and N. Kheir, "Energy management studies for a new generation of vehicles (Milestone #5: Fuzzy logic for the series hybrid)," Tech. Rep., Dept. Elect. Syst. Eng., School Eng. Comput. Sci., Oakland Univ.,Rochester, MI, Mar. 1998.

[36] N. Jalil and N. Kheir, "Energy management studies for a new generation of vehicles (Milestone #6: Fuzzy logic for the parallel hybrid)," Tech. Rep., Dept. Elect. Syst. Eng., School Eng. Comput. Sci., Oakland Univ.,Rochester, MI, Mar. 1998.

[37] Ahmed-Ali and Francoise Lamnabhi-Lagarrigue, "Sliding Observer-Controller Design for Uncertain Triangular Nonlinear Systems," *IEEE Transactions on Automatic Contro*, Vol. 44, No. 6, pp.1244-1249, June 1999.